

**SUB-HARMONIC RESONANCE, ITS STABILITY, BIFURCATION
AND TRANSITION TO CHAOS IN A CLASS OF INERTIALLY
NONLINEAR OSCILLATORS**

By

Ashraf Abdel-Majeed Al-Shalalfeh

Supervisor

Dr. Mohammed N. Hamdan, prof.

**This Thesis was submitted in Partial Fulfillment of the Requirements for the
Master's Degree of Science in Mechanical Engineering**

Faculty of Graduate Studies

The University of Jordan

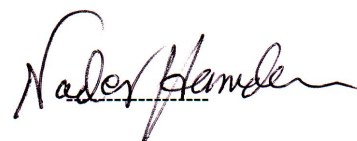
May,2005

This thesis (Sub-harmonic Resonance, Its Stability, Bifurcations And Transition To Chaos in a Class of Inertially Nonlinear Oscillators) was successfully defended and approved on May 12th, 2005.

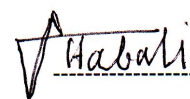
Examination Committee

Signature

Dr. Mohammed Nader Hamdan, Chairman
Prof. of Applied Mechanics - Mechanical Engineering



Dr. Saad Habali, Member
Prof. of Applied Mechanics - Mechanical Engineering



Dr. Mohammed Alkilani, Member
Assistant Prof. of Applied Mechanics - Mechanical Engineering



Dr. Mohammed Ashhab, Member
Assistant Prof. of Applied Mechanics - Mechanical Engineering
(Alhashmieh University)



ACKNOWLEDGMENT

I would like to thank first and foremost my family for giving me the chance and support to fulfill my studies. Moreover, would like to give my thanks to my colleagues & teachers in University Of Jordan that have made a year's long effort to a fun learning experience.

A grateful thank has to be addressed to Prof. Mohammed N. Hamdan that even though his tight time table always found time to help me when I needed, and for his excitement that really motivated the curiosity of me, with hope that this study won't let him down.

This study and this effort are dedicated to my father that with lifetime hard work has given me much inspiration.

DEDICATION

To My Family...

Who Built My Heart, Soul & Mind.

LIST OF CONTENTS

Subject	Page
Committee decision	ii
Acknowledgement	iii
Dedication	iv
List of contents	v
List of figures	vi
Nomenclature	viii
Abstract	ix
Introduction	1
Literature survey	10
The method of multiple scales	13
The method of harmonic balance	23
Chaos diagnostic tools	33
Results and discussion of results	40
Recommendations	59
References	60
Abstract in Arabic	65

LIST OF FIGURES

Figure 1	<i>Numerical solution</i> : $\varepsilon = 1, \varepsilon_1 = 0, \varepsilon_2 = 0.1, \delta = 0.1, P = 4,$ $\Omega = 4, u(0) = 1, \dot{u}(0) = 0.$	42
Figure 2	<i>Numerical solution</i> : $\varepsilon = 1, \varepsilon_1 = 0, \varepsilon_2 = 0.1, \delta = 0.1, P = 14,$ $\Omega = 4, u(0) = 1, \dot{u}(0) = 0.$	42
Figure 3	<i>Numerical solution</i> : $\varepsilon = 1, \varepsilon_1 = 0, \varepsilon_2 = 0.1, \delta = 0.1, P = 14,$ $\Omega = 4, u(0) = 5, \dot{u}(0) = 0.$	43
Figure 4	<i>Numerical solution</i> : $\varepsilon = 1, \varepsilon_1 = 0, \varepsilon_2 = 0.1, \delta = 0.02, P = 4,$ $\Omega = 4, u(0) = 5, \dot{u}(0) = 0.$	43
Figure 5	<i>Numerical solution</i> : $\varepsilon = 1, \varepsilon_1 = 0, \varepsilon_2 = 0.1, \delta = 0.02, P = 8,$ $\Omega = 4, u(0) = 5, \dot{u}(0) = 0.$	44
Figure 6	<i>MMS, 2MHB and Numerical solution</i> : $\varepsilon = 1, \varepsilon_1 = 0.02,$ $\varepsilon_2 = 0.2, \delta = 0.01, P = 5.$	45
Figure 7	<i>MMS, 2MHB and Numerical solution</i> : $\varepsilon = 1, \varepsilon_1 = 0.2,$ $\varepsilon_2 = 0.02, \delta = 0.01, P = 1.$	46
Figure 8	<i>MMS, 2MHB and Numerical solution</i> : $\varepsilon = 1, \varepsilon_1 = 0.1,$ $\varepsilon_2 = 0.1, \delta = 0.01, P = 1.$	46
Figure 9	<i>MMS, 2MHB and Numerical solution</i> : $\varepsilon = 1, \varepsilon_1 = 0.1,$ $\varepsilon_2 = 0.05, \delta = 0.01, P = 1.$	47
Figure 10	<i>Approximate (MMS) results</i> : $\varepsilon = 1, \varepsilon_1 = 0.02, \varepsilon_2 = 0.2,$ $\delta = 0.01, P = 5.$	48
Figure 11	<i>Approximate (MMS) results</i> : $\varepsilon = 1, \varepsilon_1 = 0.2, \varepsilon_2 = 0.02,$ $\delta = 0.01, P = 1.$	48
Figure 12	<i>Approximate MMS solution</i> : $\varepsilon = 1, \varepsilon_1 = 0.1, \varepsilon_2 = 0.1,$ $\delta = 0.01, P = 1.$	49
Figure 13	<i>Approximate 2MHB solution</i> : $\varepsilon = 1, \varepsilon_1 = 0.2, \varepsilon_2 = 0.02,$ $\delta = 0.01, P = 5.$	49
Figure 14	<i>Approximate 2MHB solution</i> : $\varepsilon = 1, \varepsilon_1 = 0.02, \varepsilon_2 = 0.2,$ $\delta = 0.01, P = 1.$	50
Figure 15	<i>Approximate 2MHB solution</i> : $\varepsilon = 1, \varepsilon_1 = 0.1, \varepsilon_2 = 0.1,$ $\delta = 0.01, P = 1.$	50

Figure 16	<i>Lyapunov exponents. $\varepsilon = 1, \varepsilon_1 = 0.02, \varepsilon_2 = 0.2, \delta = 0.01,$ $P = 5, \Omega = 3.5, u(0) = 1.75, \dot{u}(0) = 0.$</i>	51
Figure 17	<i>Numerical solution : $\varepsilon = 1, \varepsilon_1 = 0.01, \varepsilon_2 = 0.1, \delta = 0.01,$ $P = 14, \Omega = 3.14, u(0) = 5, \dot{u}(0) = 1.$</i>	52
Figure17 (d)	<i>Lyapunov exponents. $\varepsilon = 1, \varepsilon_1 = 0.01, \varepsilon_2 = 0.1, \delta = 0.01,$ $P = 14, \Omega = 3.14, u(0) = 5, \dot{u}(0) = 1.$</i>	52
Figure 18	<i>Numerical solution : $\varepsilon = 1, \varepsilon_1 = 0.1, \varepsilon_2 = 0.02, \delta = 0.01,$ $P = 8, \Omega = 1.2, u(0) = 5, \dot{u}(0) = 1$</i>	53
Figure 19	<i>Numerical solution : $\varepsilon = 1, \varepsilon_1 = 0.1, \varepsilon_2 = 0.05, \delta = 0.01,$ $P = 9, \Omega = 1.2, u(0) = 4, \dot{u}(0) = 1$</i>	53
Figure 20	<i>Numerical solution : $\varepsilon = 1, \varepsilon_1 = 0.01, \varepsilon_2 = 0.1, \delta = 0.01,$ $P = 14, \Omega = 2.84, u(0) = 5, \dot{u}(0) = 5$</i>	54
Figure 20 (d)	<i>Lyapunov exponents. $\varepsilon = 1, \varepsilon_1 = 0.01, \varepsilon_2 = 0.1, \delta = 0.01,$ $P = 14, \Omega = 2.84, u(0) = 5, \dot{u}(0) = 5.$</i>	54
Figure 21	<i>Numerical solution : $\varepsilon = 1, \varepsilon_1 = 0.01, \varepsilon_2 = 0.1, \delta = 0.01,$ $P = 14, \Omega = 2.843, u(0) = 6, \dot{u}(0) = 5$</i>	55

NOMENCLATURE

Ω	Forcing Frequency (radians)
ω	Natural frequency (radians)
δ	Damping Coefficient
σ	Detuning Parameter
P	Force Amplitude
ε	Perturbation Parameter
ε_1	Coefficient of Inertial nonlinearity
ε_2	Coefficient of Static nonlinearity
u	Displacement
v	Variation of (u)
t	Real time (sec.)
T_0	Slow time scale
T_i	Fast time scale
D_i	$\frac{\partial}{\partial T_i}$
Λ	Amplitude of generating (particular) solution
A_i, B_i	Amplitude of assumed HB solution
ϕ	Phase angle
Δ	Characteristic determinant
λ_i	Lyapunov exponents
R	Radical

**SUB-HARMONIC RESONANCE , ITS STABILITY, BIFURCATION
AND TRANSITION TO CHAOS IN A CLASS OF INERTIALLY
NONLINEAR OSCILLATORS**

By

Ashraf Abdel_Majeed Al-Shalalfeh

Supervisor

Dr. Mohamad N. Hamdan, prof.

ABSTRACT

This work presents approximate analytical and numerical investigations into the 1/3-sub-harmonic resonance response, its stability, bifurcations and transition to chaos for the class of inertially and elastically nonlinear, harmonically excited single degree of freedom oscillators described by the dimensionless equation of motion:

$$\ddot{u} + \delta\dot{u} + u + \varepsilon_1(u^2\ddot{u} + u\dot{u}^2) + \varepsilon_2u^3 = P \cos(\Omega t)$$

where $\delta, \varepsilon_1, \varepsilon_2$ and P are dimensionless positive parameters, Ω is the forcing frequency and u is the dimensionless displacement. The interest is the case where the forcing frequency is in the range where the steady state response of this oscillator is dominated by the 1/3 sub-harmonic. Approximate analytical solutions to the 1/3 sub-harmonic resonance curves are obtained, for comparison purposes, using the two modes harmonic balance (2MHB) method as well as the multiple scales (MMS) perturbation method. Stability analyses of the obtained approximate solutions were used to examine the link if any between the transition to chaos and stability limits of these approximate solutions. A number of well known numerical simulation procedures, i.e. phase plane

plots, Poincare' maps, Lyapunov exponents, frequency spectra and direct integration of equation of motion were used to verify theoretical results and observe chaotic behavior. Results of typical steady state behavior of the above oscillator are presented in graphical form for a selected range of system parameters. It is shown that first order approximate solutions, despite their limited quantitative and qualitative accuracies, when combined with relatively simple well known numerical methods, can provide a useful mean to uncover important aspects of the complicated dynamic behavior of a harmonically forced single degree of freedom nonlinear oscillator.

INTRODUCTION

1 Sub-harmonic resonance and chaos

One of the most interesting characteristics of the steady state response of a nonlinear single degree of freedom oscillator to a harmonic excitation is that the nonlinearity can generate, in addition to the usual primary harmonic component, harmonic components whose frequency Ω_p is a sub-multiple or a multiple of the harmonic excitation frequency Ω . The harmonic component whose frequency is Ω/l or $\frac{n}{l}\Omega$, is called an order $\frac{1}{l}$ sub-harmonic or an order $\frac{n}{l}$ ultra-sub-harmonic, respectively, where n, l are integers. On the other hand, a harmonic component which has a frequency $n\Omega$ is called an order n super-harmonic or, usually, an order n ultra-super-harmonic when $n \geq 4$. Depending on system parameters, nonlinearity type and range of excitation frequency, the nonlinearity can sustain a resonant, i.e large amplitude, steady state sub or super-harmonic response [1-15]. It is noted that a positively damped, linear oscillator has only a single limiting set, i.e an attractor (repellor) when positively (negatively)damped, where the whole phase space is the catchment (repelling) region. Thus regardless of the starting conditions, the steady state response of the linear oscillator to a harmonic excitation either settles into a point (periodic) attractor (if positively damped), or diverges to infinity when it is limiting set is a repellor (when the oscillator is negatively damped). In other words, in a positively damped, harmonically driven linear oscillator the steady state response is independent of the initial conditions, is harmonic with the same frequency as the excitation, the frequency response is single valued, and the free oscillation decays to

zero at the steady state. On the other hand, for a harmonically driven nonlinear oscillator the free oscillation may not decay to zero even when the oscillator is positively damped. Also at steady state the oscillator may have multiple competing (coexisting) attractors (e.g.; periodic, limit cycles, quasi-periodic, aperiodic and chaotic) each with its basin of attraction separated by repellers and saddle limiting sets [1-4]. Thus depending on the starting conditions and range of system parameters, the response of the harmonically driven nonlinear oscillator may show a drastic quantitative as well as qualitative change as one or more of its control parameters (i.e. frequency or amplitude of the harmonic excitation) goes through a critical (i.e. bifurcation) value and enters the catchment region of a nearby or a distant attractor. For example, for the classical, positively damped, harmonically driven, duffing oscillator with cubic hardening nonlinearity, the steady state response when the excitation frequency Ω is in neighborhood of the linear natural frequency ω of the oscillator (i.e. in the primary resonance region) is dominated by the fundamental harmonic. Also, in this case, the free oscillation dies out, and the frequency response curve consists of three branches: two stable branches (attractor) separated by an unstable branch (repellor). Thus, for given system parameters and excitation frequency the initial conditions play a crucial role in determining which of the two coexisting stable steady states solutions (i.e. attractors) represents the actual response of the oscillator.

Now, consider the case where the excitation frequency Ω in the above Duffing oscillator is gradually increased above the linear natural frequency ω . When Ω is increased from $\Omega \approx 3\omega$, it is possible, depending of system damping, forcing amplitude and initial conditions, for the system at steady state to sustain the free oscillation in addition to the primary steady state response, even when the oscillator is positively

damped and in contrast with the linear theory prediction. Thus , in this case, at the steady state , the cubic nonlinearity seems to adjust the frequency of free oscillation to about one third of the forcing frequency so that the total response ,which now consists of the free oscillation term (with frequency $\approx \Omega/3$, i.e. a 1/3rd sub-harmonic term) and particular term (with frequency Ω), is periodic with period τ which is about three times that of the fundamental τ_0 ; i.e. : $\tau = 3\tau_0 = \frac{6\pi}{\Omega}$. Furthermore, as the excitation frequency Ω is gradually increased from $\Omega \approx 3\omega$, the amplitude of the excited 1/3rd sub-harmonic tends to increase and that of the fundamental harmonic (i.e. amplitude of the particular solution) tends to decrease and becomes nearly equal to that of the corresponding linear oscillator , so that the steady state periodic response becomes dominated by the 1/3rd sub-harmonic component. Depending on forcing amplitude and system damping, it is possible to excite a steady state sub-harmonic response, i.e. a sub-harmonic resonant response, with magnitude much larger than that of the fundamental response. In other words, the oscillator now has in addition to the fundamental attractor another coexisting distant (i.e. of larger amplitude) sub-harmonic attractor. Thus , depending on initial conditions , a steady state fundamental response of relatively small amplitude may lose stability and moves to a sub-harmonic attractor with much larger amplitude as a system parameter, i.e. excitation amplitude, goes through a critical bifurcation value leading to violent large amplitude vibrations. This sudden and sub-critical loss of stability of a dynamical system operating above primary resonance region has been reported in several practical engineering systems; i.e., (see Nayfeh and Mook [1]) an airplane engine running at an angular speed much larger than that of the airplane parts natural frequencies was reported to lead under certain operating conditions to violent vibrations of some of these parts.

It is noted that for a frequency of excitation Ω below the oscillator linear frequency ω , it is possible, depending on initial conditions and system parameters, to excite a super-harmonic resonant response, again due to the fact that, like in the case of sub-harmonic resonance region, the free oscillation term in the total solution may not decay to zero even when the nonlinear oscillator is positively damped [1]. Thus, for example, for the positively damped, harmonically driven Duffing oscillator with cubic hardening static nonlinearity, a super-harmonic resonance may get excited for the right system parameters and initial conditions when Ω is in the range $\Omega \approx \frac{1}{3}\omega$. However, the super-harmonic resonance response, unlike the sub-harmonic one, has the same period as the excitation; its amplitude usually grows steadily from a negligible value to a value comparable or larger than that of the fundamental harmonic without any bifurcation.

It should be borne in mind that a key aspect of the steady state response of a nonlinear single degree of freedom to harmonic excitation, i.e. primary and secondary resonances, discussed above is that they are periodic. The classical theory postulate that a nonlinear, positively damped, single degree of freedom oscillator subjected to a periodic (i.e. harmonic) excitation will always have a periodic steady state output, has been challenged since 1970's by the new theory of chaotic motions. During the last three decades numerical simulation studies and experimental investigations have shown that the nonlinear oscillator may possess solutions which were not only aperiodic, but which also have a noisy (i.e. random-like) behavior. It is noted that not all of obtained analytic periodic solutions of a nonlinear oscillator are stable (attractors). Also, as indicated above, it is possible that some of coexisting attractors are non-periodic (i.e. chaotic) which cannot be uncovered using the approximate analytical methods of nonlinear theory. Consequently, recent research efforts aiming at obtaining a realistic

assessment of a nonlinear system dynamics and synthesis of a reliable control strategy tend to carry out a detailed stability and bifurcation analyses to uncover various possible dynamic systems bounded periodic, aperiodic, chaotic and unbounded motions. Methods used to carry out such tasks, which usually are rather elaborate even when the analysis is only carried out to first order, are a combination of approximate analytic, geometric and numeric methods, [1-4, 16-23]. Each of these methods has its advantages and drawbacks; a detailed discussion of these techniques goes beyond the scope of this overview and can be found somewhere else, e.g. [1, 2, 16-18]. Stability analysis and numerical simulation studies of sub-harmonic resonance in various types of harmonically excited Duffing oscillators have shown that chaotic motions are associated with the loss of stability of a sub- or super- harmonic resonance, i.e. one characteristic precursor to chaotic motions is the appearance and then loss of stability of a sub- or super-harmonic resonance, e.g. [19-22, 24-31]. Studies dealing with approximate analytic-numeric stability and bifurcation analyses of sub-harmonic resonance and its transition to chaos in single degree of freedom nonlinear oscillators have to the author's best knowledge, been limited , except in few cases, to first order approximations and to statically stable and unstable oscillators with only static nonlinearity [25 -31]. These studies have shown that the zone of a chaotic motion in the response of various types of the classical duffing oscillator is found as a transition zone between a secondary (sub-or-super-harmonic) resonance solution and the corresponding fundamental harmonic solution in the neighborhood of points of vertical tangency (the stability limits) on the sub-(super)-harmonic resonance. Consequently, several efforts have been made to analytically seek a link between stability limits of sub-harmonic solutions and the onset of chaotic motions [25-29]. In fact one of the most celebrated scenario for chaotic motion development is the continuous sequence of periodic doubling ($1/2$ sub-

harmonic) bifurcations [19-22]. In this scenario, as a system control parameter, i.e. forcing frequency or forcing amplitude, is changed a periodic response, i.e. a period T motion, undergoes a bifurcation or change to another period $2T$ motion, i.e. the new motion has twice the period of the original motion. As the control parameter is changed further, the oscillator period $2T$ motion bifurcates to a period $4T$ motion; then the $4T$ motion bifurcates to $8T$ motion...etc. This bifurcation scenario continues until the control parameter reaches a critical value (defined by Feigenbaum scaling rule, see, i.e., [19-21]) beyond which the oscillator motion may become chaotic. Furthermore, numerical simulation results have shown some chaotic attractors in several nonlinear systems to contain windows (pockets) of stable sub-harmonic orbits, e.g. [19, 24]. This led to some authors' view [19]: "some chaotic attractors are in fact nothing but an ensemble of many long sub-harmonics, whose basins are so small and close together that the slightest amount of noise moves experimentally observed trajectories from one sink to another, giving the appearance of chaos". Finally, it is noted that sub-harmonics provide a useful means in basic electromechanical timing mechanisms to gear down in stages from a high frequency electrical input to a low frequency output appropriate for a mechanical drive [2].

In summary, the study of stability and bifurcations of the sub-harmonic resonance response in nonlinear oscillators are crucial due the following facts:

- 1- A dynamic system operating in the sub-harmonic resonance region (i.e. at high rotational speed) may undergo a sub-critical loss of stability to a violent and destruction sub-harmonic vibrations.
- 2- The appearance of sub-harmonics and their stability loss are associated with the possibility of generating aperiodic and chaotic steady state motions.

2 Objective of the thesis

In light of the above overview , this research aims at obtaining analytical approximations to the $1/3^{\text{rd}}$ sub-harmonic resonance response and studying its stability, bifurcations and transition to chaos , in the class of harmonically driven oscillators with inertial and elastic symmetric nonlinearities:

$$\ddot{u} + \delta \dot{u} + u + \varepsilon_1 (u^2 \ddot{u} + u \dot{u}^2) + \varepsilon_2 u^3 = P \cos(\Omega t) \quad (1)$$

Where $\delta, \varepsilon_1, \varepsilon_2$ and P are dimensionless positive parameters, Ω is the forcing frequency and u is the dimensionless displacement. The interest is the case where the forcing frequency is in the range where the steady state response of this oscillator is dominated by the $1/3$ sub-harmonic. Approximate analytical solutions to the $1/3$ sub-harmonic resonance curves are obtained, for comparison purposes, using the two modes harmonic balance (2MHB) method as well as the multiple scales (MMS) perturbation method. Stability analyses of the obtained approximate solutions are used to examine the link if any between the transition to chaos and stability limits of these approximate solutions. A number of well known numerical simulation procedures, i.e. phase plane plots, Poincare' maps, Lyapunov exponents, frequency spectra and direct integration of equation of motion are used to verify theoretical results and observe chaotic behavior.

Results of typical steady state behavior of the above oscillator are presented in graphical form for a selected range of system parameters. It is shown that first order approximate solutions, despite their limited quantitative and qualitative accuracies, when combined with relatively simple well known numerical methods , can provide a useful mean to uncover important aspects of the complicated dynamic behavior of a harmonically forced single degree of freedom nonlinear oscillator.

3 Significance of this work

The interest in the nonlinear dynamic response of the class of oscillators governed by equation (1) lies in the different physical systems that it models, such as the in-plane flexural vibrations of an in- extensible non-rotating and rotating beam element [32-35]. The demands in modern machinery designs for lighter weight, higher flexibility and higher operating speeds (i.e. speeds above the fundamental natural frequency) makes such highly flexible and light machine elements susceptible to "dangerous sub-harmonic resonances. Also the design of a proper strategy to control the motions and suppress the vibrations of such machine elements requires carrying out a detailed stability and bifurcation analyses to uncover their various possible dynamic behaviors. Furthermore, as indicted in the previous section, most of the existing theoretical analyses of sub-harmonic resonances deal with oscillators with static hardening or static softening nonlinearities. On the other hand, the above oscillator includes both hardening and inertial softening nonlinearities, where each of these nonlinearities alone leads to qualitatively different frequency characteristics.

Direct numerical integration and basic methods of Lyapunov exponents, Poincare maps, frequency analysis and phase plane plots will be used to check the validity of the obtained approximate analytic results and examine system chaotic behaviors.

4 Layout of this Thesis

This thesis is divided into seven chapters. The first chapter is an introduction. It provides an overview of the importance of studying sub-harmonic resonance and its association to chaotic motion. Also, this chapter includes the thesis objectives and layout. Chapter (2) presents a review of relevant literature. Chapter (3) includes the approximate analytic solution obtained using the harmonic balance method and its stability analysis. The analytic solution obtained using the method of Multiple-Scales (MMS) and its stability analysis are given in Chapter (4). Chapter (5) includes a summary of the methods used for chaos detection. The obtained theoretical and numerical results are presented and discussed in Chapter (6). In Chapter (7) conclusions and recommendations of this work are presented.

LITERATURE SURVEY

1 Introduction

The study of sub-harmonic resonance response and its stability analysis in single degree of freedom systems under harmonic excitation have been treated in several textbooks, e.g. [1-4], and in a number of investigations, e.g. [5-15]. The Duffing type oscillators were treated in [1-12], oscillators with piecewise non-symmetric characteristics were treated in [13], a Duffing oscillator with hardening static and inertia nonlinearities was treated in [14], and a Mathieu-Duffing type oscillator was treated in [15]. The approximate solutions to the sub-harmonic resonance were obtained using various analytical and numerical techniques; i.e., the method of the multi-scales (MMS) was used in [1], the harmonic balance method was used in [2-9], a harmonic balance- "suitable parametric form" procedure was used in [10], a generalized perturbation method was used in [14], and the method of normal forms was used in [15].

The qualitative geometric theory techniques, frequently used in the analysis of nonlinear dynamical systems, periodic, aperiodic and chaotic motions are described, among others, in [19-23]). These techniques along with various approximate analytic methods and aided with numerical simulations has been used in many investigations concerned with analysis of stability and bifurcations of sub- and ultra-sub-harmonic resonance responses and transition to chaotic motions in harmonically forced single degree of freedom nonlinear systems, e.g.[25-31]. Szemplinska- Stupnika [27, 28] used the harmonic balance, floquet theory and computer simulations to study stability and bifurcations of sub-harmonic resonance and transition to chaos in symmetric and asymmetric Duffing oscillators. The presented results in these studies revealed that

chaotic motion occurs in transition zones between two periodic solutions having different periods (having different topological properties), e.g. between a sub-or a ultra sub-harmonic and a fundamental solution). That is, these studies have shown that the chaotic motion in a symmetric or asymmetric Duffing oscillators of the hardening type, the chaotic motion is always associated with loss of stability of secondary (i.e. sub- or ultra-sub-harmonic or super-harmonic) resonance response. The above approach was also used by Janicki and Szemplinska-Stupnicka [24-25] to study sub-harmonic resonance and develop a criterion for the onset of chaos in single degree of freedom oscillators with static nonlinearities under harmonic excitation. The harmonic balance aided with analog and numerical simulations was used by Hayashi [29] to analyze the stable and unstable manifolds, solution branching , homoclinic tangle of the fundamentally nonlinear , hardening type, Duffing oscillator known as Duffing-Uda oscillator. Hamdan and Nayfeh [30] , and Nayfeh et al [31] respectively used a first order and a second order Multiple-Scales method (MMS) solutions to the $1/2$ subharmonic resonance, a Floquet stability analysis of the obtained approximate solutions, and numerical simulation to study the onset of period doubling bifurcations and transition to chaos in a single machine quasi-infinite busbar system. The system was modeled as a Mathieu's oscillator with quadratic and cubic nonlinearities and external harmonic excitation. Their results showed that the loss of stability of the obtained approximate solutions agrees fairly well (more accurately when using the second order solution) with the onset of period-doubling bifurcations which is a precursor to chaos and loss of synchronism.

Al-Qaisia and Hamdan [35, 36] studied the period doubling and transition to chaos in the oscillator in equation (1) using the harmonic balance Floquet stability analysis of asymmetric and symmetric approximate solutions for the fundamental

resonance and numerical simulations. They proposed a criterion for the onset of period doubling in this class of oscillators based on the intersection of the approximate symmetric and asymmetric harmonic balance solutions.

In summary, approximate analytic solutions to sub- and ultra-sub-harmonic resonances, their stability analysis and their association to period doubling, onset of chaos, and loss of synchronism on single degree of freedom nonlinear oscillators under harmonic excitation have been the subject of numerous investigations. These investigations have for the most part considered the cases where the oscillator has a hardening or softening nonlinearities. The class of oscillators in equation (1) which includes both hardening and softening; i.e. elastic and inertial , nonlinearities appears to have not been considered except in [35,36], where the analyses was concerned only with the primary resonance response.

THE METHOD OF MULTIPLE SCALES (MMS)

1 The Method of Multiple Scales (MMS)

The multiple scales method, (MMS), is one of the most commonly used procedures for analyzing various resonances in weakly nonlinear systems. The underlying idea and procedural steps of this method are described in several textbooks, i.e. Nayfeh and Mook[1]. This method uses a number of time scales and power series expansion of the dependent variable and system parameters to convert the nonlinear system equation of motion into a hierarchical set of linear partial differential equation. This expansion is based on a small positive gage parameter ε usually intentionally introduced by a scaling procedure depending on the type of sought periodic solution (i.e. primary or secondary resonance response). The obtained hierarchical set of linear partial differential equations are then solved consecutively to the desired order of approximation. The main advantages of this method include its applicability for a wide class of nonlinear systems, and it has systematic procedural steps. This procedure however is restricted to weakly nonlinear systems, algebraically cumbersome when solutions are carried to second and higher order approximations and it involves some heuristic procedures at the second and higher order which can introduce extraneous solutions (periodic solutions which do not exist in the system being analyzed), e.g., see [16,17].

This chapter includes the first order MMS approximate solutions for the 1/3 sub-harmonic resonance response in the oscillator described by equation (1). It also includes a local stability analysis of the obtained approximate solutions.

2 First-Order MMS Approximation

In applying the MMS method to the analysis of a sub-harmonic response of a nonlinear oscillator, such as the one under consideration given by equation (1), one must keep in mind that the sub-harmonic resonance is, as indicated in section (1-1) is a bifurcation phenomenon. That is, the $1/3$ sub-harmonic resonance response of equation (1) arises as a bifurcation from a generating fundamental response (a periodic response having the same as that of the harmonic forcing). Furthermore the order (i.e. scaling) scheme used when applying the MMS method will depend on the type of the periodic response sought [1]. In order to obtain a fundamental harmonic generating solution for the sub-harmonic resonance response, it is necessary to order the equation of motion so that the forcing term appears at the lowest (e.g. zero) order, and the damping and nonlinear terms appear at the next higher order in the hierarchical set of equations. Accordingly, equation (1) is rewritten in the reordered form:

$$\ddot{u} + \varepsilon \delta \dot{u} + u + \varepsilon \varepsilon_1 (u^2 \ddot{u} + u \dot{u}^2) + \varepsilon \varepsilon_2 u^3 = P \cos(\Omega t) \quad (2)$$

Where $0 < \varepsilon < 1$. One then defines a fast time scale $T_0 = t$, on which the main oscillatory response occurs, and slow time scales $T_n = \varepsilon^n t$, $n \geq 1$, on which phase and amplitude modulation takes place. In terms of these time scales, the time derivatives become:

$$\begin{aligned} \frac{d}{dt} &= D_0 + \varepsilon D_1 + \varepsilon^2 D_2 + \dots \\ \frac{d^2}{dt^2} &= D_0^2 + 2\varepsilon D_0 D_1 + \varepsilon^2 (2D_0 D_2 + D_1^2) + \dots \end{aligned} \quad (3)$$

Where $D_n = \frac{\partial}{\partial T_n}$. Also one assumes a power series expansion for the dependent

variable u in the form:

$$u(t, \varepsilon) = u_0(T_0, T_1, T_2) + \varepsilon u_1(T_0, T_1, T_2) + \varepsilon^2 u_2(T_0, T_1, T_2) \quad (4)$$

Since the 1/3 sub-harmonic resonance response is sought, a detuning parameter σ ,

which expresses the nearness of Ω to 3ω , may be introduced according to [31]:

$$1 = \omega^2 = \frac{1}{9}\Omega^2 + \varepsilon\sigma \quad (5)$$

Substituting equations (3)-(5) into equation (2) one obtains:

$$\begin{aligned} & (D_0^2 + 2\varepsilon D_0 D_1 + 2\varepsilon^2 D_0 D_2 + \varepsilon^2 D_1^2)(\varepsilon u_1 + \varepsilon^2 u_2 + \varepsilon^3 u_3) \\ & + \varepsilon \delta (D_0 + \varepsilon D_1 + \varepsilon^2 D_2)(\varepsilon u_1 + \varepsilon^2 u_2 + \varepsilon^3 u_3) \\ & + \left(\frac{1}{9}\Omega^2 + \varepsilon\sigma\right)(\varepsilon u_1 + \varepsilon^2 u_2 + \varepsilon^3 u_3) \\ & + \varepsilon \varepsilon_1 \left\{ (\varepsilon u_1 + \varepsilon^2 u_2 + \varepsilon^3 u_3)^2 [(D_0^2 + 2\varepsilon D_0 D_1 + 2\varepsilon^2 D_0 D_2 + \varepsilon^2 D_1^2)(\varepsilon u_1 + \varepsilon^2 u_2 + \varepsilon^3 u_3)] \right. \\ & \quad \left. + (\varepsilon u_1 + \varepsilon^2 u_2 + \varepsilon^3 u_3) [(D_0 + \varepsilon D_1 + \varepsilon^2 D_2)(\varepsilon u_1 + \varepsilon^2 u_2 + \varepsilon^3 u_3)]^2 \right\} \\ & + \varepsilon \varepsilon_2 [\varepsilon u_1 + \varepsilon^2 u_2 + \varepsilon^3 u_3]^3 = P \cos(\Omega t) \quad (6) \end{aligned}$$

Equating coefficients of different powers of ε in equation (6) to zero leads to following set of linear partial differential equations:

ε^0 :

$$D_0^2 u_0 + \frac{1}{9}\Omega^2 u_0 = P \cos(\Omega t) \quad (7)$$

ε^1 :

$$D_0^2 u_1 + \frac{1}{9}\Omega^2 u_1 = -\sigma u_0 - \varepsilon_1 u_0 (D_0 u_0)^2 - \varepsilon_2 u_0^3 - \delta D_0 u_0 - 2D_0 D_1 u_0 - \varepsilon_1 u_0^2 D_0^2 u_0 \quad (8)$$

ε^2 :

$$\begin{aligned}
D_o^2 u_2 + \frac{1}{9} \Omega^2 u_2 = & -\sigma u_1 - D_1^2 u_o - 2D_o D_2 u_o - 2\varepsilon_2 u_o^2 - \varepsilon_1 u_o^2 D_o^2 u_1 - 2\varepsilon_1 u_o^2 D_o D_1 u_o \\
& - \varepsilon_1 u_o u_1 D_o^2 u_o - 2\varepsilon_1 u_o D_o u_1 D_o u_o - 2\varepsilon_1 u_o D_1 u_o D_o u_o - \delta D_1 u_o \\
& - \varepsilon_1 u_1 (D_o u_o)^2 - \varepsilon_2 u_1 u_o^2 - \delta D_o u_1 - 2D_o D_1 u_1 - \varepsilon_1 u_o u_1 D_o^2 u_o
\end{aligned} \quad (9)$$

The solution of equation (7) can be expressed in either the form

$$u_o = a(T_1, T_2) \cos\left[\frac{1}{3}\Omega T_o + \beta(T_1, T_2)\right] + 2\Lambda \cos(\Omega T_o)$$

(10)

Or the form

$$u_o = A(T_1, T_2) e^{1/3(i\Omega T_o)} + \bar{A}(T_1, T_2) e^{-1/3(i\Omega T_o)} + \Lambda e^{i\Omega T_o} + \Lambda e^{-i\Omega T_o}$$

(11)

Where \bar{A} is the complex conjugate of $A = \frac{1}{2} a e^{i\beta}$ and

$$\Lambda = -\frac{9P}{16\Omega^2}.$$

(12)

Substituting equation (11) into equation (8) leads to

$$\begin{aligned}
D_o^2 u_1 + \frac{1}{9} \Omega^2 u_1 = & \left[-\frac{2}{3} i D_1 A - \frac{1}{3} i \delta \Omega A - \sigma A + \left(\frac{2}{9} \Omega^2 \varepsilon_1 - 3\varepsilon_2 \right) A^2 \bar{A} \right. \\
& \left. + \left(\frac{2}{3} \Omega^2 \varepsilon_1 - 3\varepsilon_2 \right) \bar{A}^2 \Lambda + \left(\frac{20}{9} \Omega^2 \varepsilon_1 - 6\varepsilon_2 \right) \Lambda^2 A \right] e^{1/3(i\Omega T_o)} \\
& + \left[-i\delta\Omega\Lambda - \sigma\Lambda + \left(\frac{2}{9} \Omega^2 \varepsilon_1 - \varepsilon_2 \right) A^3 + \left(\frac{20}{9} \Omega^2 \varepsilon_1 - 6\varepsilon_2 \right) A^2 \Lambda + (2\varepsilon_1 \Omega^2 - 3\varepsilon_2) \Lambda^3 \right] e^{i\Omega T_o} \\
& + \left[(2\varepsilon_1 \Omega^2 - 3\varepsilon_2) A^2 \Lambda + \left(\frac{14}{9} \varepsilon_1 \Omega^2 - 3\varepsilon_2 \right) \bar{A} \Lambda^2 \right] e^{5/3(i\Omega T_o)} \\
& + \left[\left(\frac{26}{9} \varepsilon_1 \Omega^2 - 3\varepsilon_2 \right) \Lambda^2 A \right] e^{7/3(i\Omega T_o)} + (2\varepsilon_1 \Omega^2 - \varepsilon_2) \Lambda^3 e^{i3\Omega T_o} + cc
\end{aligned} \quad (13)$$

Where cc stands for the complex conjugate of the preceding terms. Eliminating the secular terms (terms that render the expansion non-uniform for large t) in equation (13), one obtains:

$$-\frac{2}{3}iD_1A - \frac{1}{3}i\delta\Omega A - \sigma A + \left(\frac{2}{9}\varepsilon_1\Omega^2 - 3\varepsilon_2\right)A^2\bar{A} + \left(\frac{2}{3}\varepsilon_1\Omega^2 - 3\varepsilon_2\right)\bar{A}^2\Lambda + \left(\frac{20}{9}\varepsilon_1\Omega^2 - 6\varepsilon_2\right)\Lambda^2A = 0 \quad (14)$$

Noting that:

$$A = \frac{1}{2}ae^{i\beta}, \quad \bar{A} = \frac{1}{2}ae^{-i\beta}, \quad a = a(T_1, T_2, \dots), \quad \beta = \beta(T_1, T_2, \dots),$$

$$D_1A = A' = \frac{a'}{2}e^{i\beta} + i\frac{a}{2}\beta'e^{i\beta}, \quad e^{\pm i3\beta} = \cos(3\beta) \pm i\sin(3\beta), \text{ and after factoring out } e^{i\beta},$$

equation (14) becomes

$$-\frac{1}{3}ia' + \frac{1}{3}a\beta' - \frac{a\sigma}{2} - \frac{1}{6}i\delta\Omega a + \left(\frac{2}{9}\varepsilon_1\Omega^2 - 3\varepsilon_2\right)\frac{a^3}{8} + \left(\frac{20}{9}\varepsilon_1\Omega^2 - 6\varepsilon_2\right)\frac{a\Lambda^2}{2} + \left(\frac{2}{3}\varepsilon_1\Omega^2 - 3\varepsilon_2\right)\frac{\Lambda a^2}{4}(\cos(3\beta) - i\sin(3\beta)) = 0 \quad (15)$$

Where a prime denotes derivative with respect to the slow time T_1 . Separating the real and imaginary parts of the complex differential equation (15) and equating each to zero, leads to the amplitude and phase modulation first order real differential equations in the time T_1 :

$$a' = \frac{3}{4}\Lambda a^2(3\varepsilon_2 - \frac{2}{3}\varepsilon_1\Omega^2)\sin(3\beta) - \frac{1}{2}\delta\Omega a \quad (16)$$

$$a\beta' = \frac{3}{2}\sigma a + \frac{3}{8}(3\varepsilon_2 - \frac{2}{9}\varepsilon_1\Omega^2)a^3 + \frac{3}{4}(3\varepsilon_2 - \frac{2}{3}\varepsilon_1\Omega^2)\Lambda a^2 \cos(3\beta) + (9\varepsilon_2 - \frac{10}{3}\varepsilon_1\Omega^2)\Lambda^2 a. \quad (17)$$

The steady state motions are obtained from equations (16) and (17) by setting

$a' = \beta' = 0$; this leads to the trivial steady state solution $a = 0$ and the nontrivial steady state solutions defined by the algebraic equations:

$$\delta\Omega = \frac{3}{2}\Lambda a^2 (3\varepsilon_2 - \frac{2}{3}\varepsilon_1\Omega^2) \sin(3\beta) \quad (18)$$

$$\frac{3}{2}\sigma + \frac{3}{8}(3\varepsilon_2 - \frac{2}{9}\varepsilon_1\Omega^2)a^2 + (9\varepsilon_2 - \frac{10}{3}\varepsilon_1\Omega^2)\Lambda^2 = \frac{3}{4}(3\varepsilon_2 - \frac{2}{3}\varepsilon_1\Omega^2)\Lambda a \cos(3\beta) . \quad (19)$$

Squaring and adding equation (18) and equation (19) leads to the frequency-response equation:

$$a^4 + R_1 a^2 + R_2 = 0$$

(20)

Which has the roots:

$$a_{1,2}^2 = \frac{-R_1}{2} \pm [(\frac{R_1}{2})^2 - R_2]^{1/2}$$

(21)

Where

$$R_1 = \frac{2m_0 m_1 - m_2}{m_0^2}, \quad R_2 = \frac{m_1^2 + m_3}{m_0^2},$$

$$m_0 = \frac{3\varepsilon_2 - 2\varepsilon_1 + 2\varepsilon\varepsilon_1\sigma}{8}, \quad m_1 = \frac{\sigma}{2} + \frac{\Lambda^2}{2}(6\varepsilon_2 - 20\varepsilon_1\varepsilon_2 + 20\varepsilon\varepsilon_1\sigma),$$

(22)

$$m_2 = (\frac{\Lambda}{4})^2 (3\varepsilon_2 - 6\varepsilon_1 + 6\varepsilon\varepsilon_1)^2, \quad m_3 = \frac{\delta^2\Omega^2}{36}$$

and σ, Λ are as defined in equations (5) and (12). Equation (21), for given system parameters $\delta, \varepsilon, \varepsilon_1, \varepsilon_2, P$ and frequency Ω yields two real values (non-trivial

solutions) for the amplitude a of the 1/3 sub-harmonic resonance response of equation

$$(2) \text{ provided that } R_1 < 0, \frac{R_1^2}{4} - R_2 > 0 \text{ and } \left[\frac{R_1^2}{4} - R_2\right]^{1/2} < -\frac{R_1}{2}.$$

And a single solution (real value for a) exists provided that $\frac{R_1^2}{4} - R_2 > 0$ and

$$\left[\frac{R_1^2}{4} - R_2\right]^{1/2} > -\frac{R_1}{2}, \text{ while no solutions (no real values of } a \text{) exist when none of these}$$

conditions is satisfied.

For convenience, the steady state 1/3 sub-harmonic resonance curves of the oscillator in equation (3) obtained using the above results over a range of system parameters are presented and discussed in chapter (6). All of the needed calculations in the above equations were carried out using a specially formulated MATLAB program. The stability analysis of these solutions is presented in the next section.

3 Stability analysis

It is necessary to carry out a stability analysis of approximate steady state analytic solutions of a nonlinear system since not all of these solutions may be physically releasable (e.g. are stable). Also a key aim of the present work is to examine the relation, if any, between loss of stability of the obtained 1/3 sub-harmonic resonance solutions and the onset of chaotic motions. The local stability of steady state solutions (e.g. singular points of equations (16) and (17), describing the 1/3 sub-harmonic resonance response of the oscillator in equation (2) can be determined by imposing perturbations on these solutions; that is, one lets:

$$a = a_0 + a_1, \quad \beta = \beta_0 + \beta_1 \quad (24)$$

Where the subscript 0 denotes a steady state value and a subscript 1 denotes a perturbation (e.g. small) value. Substituting equation (24) into equations (16) and (17), after factoring out a from equation (17), using equations (18) and (20) (with a replaced by a_0 , and β replaced by β_0), and keeping only linear terms, leads to

$$a_1' = [3\alpha_1 a_0 \sin \beta_0 - \frac{\delta \Omega}{2}] a_1 + (3\alpha_1 a_0^2 \cos 3\beta_0) \beta_1 \quad (25)$$

$$\beta_1' = (2\alpha_2 a_0) a_1 - (3a_0 \alpha_1 \sin 3\beta_0) \beta_1 \quad (26)$$

Where

$$\alpha_1 = \frac{3\Lambda}{4} (3\varepsilon_2 - \frac{2}{3} \varepsilon_1 \Omega^2) , \quad \alpha_2 = \frac{3}{8} (3\varepsilon_2 - \frac{2}{9} \varepsilon_1 \Omega^2) ,$$

$$\alpha_3 = (9\varepsilon_2 - \frac{10}{3} \varepsilon_1 \Omega^2) \Lambda^2 \quad (27)$$

With, from equations (18) and (19),

$$\sin 3\beta_0 = \frac{\delta \Omega}{2a_0 \alpha_1} \quad (28)$$

$$\cos 3\beta_0 = -\frac{1.5\sigma + \alpha_3 + \alpha_2 a_0^2}{\alpha_1 a_0} . \quad (29)$$

And σ, Λ are as defined in equations (5) and (12). Equations (25) and (26) is a set of two coupled, homogeneous, ordinary linear first order differential equations, in the slow time T_1 , with constant coefficients. The solution to these equations takes the exponential form:

$$a_1 = a_{10} e^{\lambda T_1} , \quad \beta_1 = \beta_{10} e^{\lambda T_1} \quad (30)$$

Where a_{10}, β_{10} and λ are constants. Substituting the expressions in equation (30) and their first derivative into equations (25) and (26), factoring out $e^{\lambda T_1}$ leads to the algebraic homogenous (e.g. eigen value) problem:

$$\begin{bmatrix} A-\lambda & B \\ C & D-\lambda \end{bmatrix} \begin{Bmatrix} a_{10} \\ \beta_{10} \end{Bmatrix} = \begin{Bmatrix} 0 \\ 0 \end{Bmatrix} \quad (31)$$

Where A, B, C, D are constant coefficients defined as follows:

$$A = 3\alpha_1 a_0 \sin \beta_0 - \frac{\partial \Omega}{2}, \quad B = 3\alpha_1 a_0^2 \cos 3\beta_0, \quad (32)$$

$$C = 2\alpha_2 a_0, \quad D = -3a_0 \alpha_1 \sin 3\beta_0.$$

For a nontrivial solution the determinant of the coefficient matrix in the above equation must vanish. This leads to a quadric algebraic equation for the eigen value λ .

The two roots of this equation are given by:

$$\lambda_{1,2} = \frac{1}{2} \left(A + D \pm [(A + D)^2 - 4(AD - BC)]^{1/2} \right). \quad (33)$$

Then for stability of the singular points of equations (16) and (17) (i.e. steady state solutions a_0, β_0) requires the real part of the roots $\lambda_{1,2}$ in equation (33), when these roots are complex, to be negative, and these roots to be negative when they are real. That is for stability of the steady state solutions the following conditions must be satisfied:

$$A + D < 0, \quad AD - BC > 0, \quad (34)$$

Where at the stability limits the above conditions become:

$$A + D = 0, \quad AD - BC = 0. \quad (35)$$

Substituting the expressions given in equations (32) into the first of equations (35) leads to the following stability limit condition:

$$\varepsilon_1 \leq \frac{9}{2} \varepsilon_2 \Omega^2 \quad (36)$$

That is, the obtained 1/3 sub-harmonic resonance solution obtained in section (2), (e.g. given by equation (22)), is stable provided that equation (36) is satisfied.

Similarly, upon substituting the expressions defined in equations (32) into the second stability limit condition given in equation (35), leads to the following 4- the order algebraic equation in the amplitude a_0 of the 1/3 sub-harmonic steady state resonance response:

$$a_0^4 + \left(\frac{\alpha_3 + 1.5\sigma}{\alpha_2}\right)a_0^2 - \left(\frac{\delta\Omega}{2\alpha_2}\right)^2 = 0 \quad (37)$$

The roots of the above equation are given by:

$$a_0^2 = \frac{1}{2} \left[-b \pm (b^2 + 4c)^{1/2} \right] \quad (38)$$

Where

$$b = \frac{\alpha_3 - 1.5\sigma}{\alpha_2}, \quad c = \left(\frac{\delta\Omega}{2\alpha_2}\right)^2 \quad (39)$$

The real roots of the above equation define, for given system parameters of the oscillators in equation (2), the amplitude- frequency curve(s) which separate(s) the stable and unstable regions in the corresponding steady state 1/3 sub-harmonic resonance response of this oscillator. All of the calculations needed to plot these curved were carried out using a specially written MATLAB program. For convenience, examples of these results are presented and discussed in Chapter (6).

THE METHOD OF HARMONIC BALANCE (HB)

1 Introduction

The analysis of dynamic response of a nonlinear system usually involves comparisons of the results obtained using a selected approximate analytic method with those obtained numerically as well as with those obtained using other known approximate analytic methods. Such comparisons are usually necessary in order to establish confidence in the obtained results. In the previous Chapter (2), approximate analytical solutions for the $1/3$ the sub-harmonic resonance response of the oscillator in equation (1) were obtained using the well known multiple scales (MMS). In this chapter analytical approximate solutions to this problem are obtained, for comparison purposes, using the harmonic balance (HB) [2,3] which is another commonly used analytic method. The underlying idea of the HB method is that one substitutes an assumed truncated Fourier series approximation for the dependent variable in the equation of motion. Then one equates the coefficients of each of the different n lowest harmonics in the resulting equation to zero, where n is equal to the number terms in the assumed series approximation. This leads to a system of n coupled nonlinear algebraic equations in the coefficients of the assumed series which must be solved simultaneously. The HB method is usually called m modes harmonic balance, i.e. (mHB), where m is equal to the number of harmonics with different frequency in the assumed series solution. The harmonic balance (HB) method has several advantages in comparison with other well known approximate analytic methods. In addition of being probably the simplest technique, the advantages of the HB method over other methods include [17, 18]:

- 1- The harmonic balance (HB) method is not restricted to weakly nonlinear systems. For a smooth system the HB solution always converges to the exact solution provided that enough harmonics are included in the assumed truncated Fourier series approximation.
- 2- The HB method accommodates qualitative as well as quantitative changes in the approximate solution as more harmonics are included in the assumed Fourier series approximation. In other words, higher degree of accuracy can be obtained if modern appropriate numerical and symbolic computational resources such as MATLAB symbolic tool boxes are used.

In the present work, the two-mode harmonic balance (2HB) method will be used to obtain an approximate solution for the $1/3$ sub-harmonic resonance response of the oscillator in equation (1). This chapter also includes stability analysis of the obtained 2HB solution.

2 Two Modes Harmonic Balance (2MHB)

In applying the harmonic balance to obtain a steady state response of a harmonically driven single degree of freedom nonlinear system such as the oscillator in equation (2) a phase shift is usually introduced in the harmonic forcing. This is done so that the part of the assumed solution at the forcing frequency involves only a single fundamental sine or cosine term. This procedural step reduces the number of nonlinear algebraic equations in the coefficients of the assumed series solution which one has to solve to a number which is one less that would be obtained otherwise. It is also noted

that in applying the HB method, unlike the case when MMS is used, it is not necessary to reorder terms, or introduce appropriate detuning, in the nonlinear equation of motion. Accordingly, introducing a phase ϕ in the harmonic excitation of equation (1), this equation becomes:

$$\ddot{u} + \delta\dot{u} + u + \varepsilon_1(u^2\ddot{u} + u\dot{u}^2) + \varepsilon_2u^3 = P \cos(\Omega t + \phi) \quad (40)$$

A two modes harmonic approximation to the steady state 1/3 sub-harmonic resonance response of the above oscillator takes the form:

$$u(t) = A_1 \cos(\Omega t) + A_{1/3} \cos\left(\frac{\Omega t}{3}\right) + B_{1/3} \sin\left(\frac{\Omega t}{3}\right) \quad (41)$$

Where, as was indicated in chapter (1), since the sub-harmonic resonance is a bifurcation phenomenon, then, like the MMS solution, a generating fundamental term, $A_1 \cos(\Omega t)$ must be included in the assumed HB solution. Substituting equation (41) and its first and second derivatives, which are:

$$\dot{u}(t) = \Omega \left[-A_1 \sin(\Omega t) - \frac{A_{1/3}}{3} \sin\left(\frac{\Omega t}{3}\right) + \frac{B_{1/3}}{3} \cos\left(\frac{\Omega t}{3}\right) \right], \quad (42)$$

$$\ddot{u}(t) = -\Omega^2 \left[A_1 \cos(\Omega t) - \frac{A_{1/3}}{9} \cos\left(\frac{\Omega t}{3}\right) + \frac{B_{1/3}}{9} \sin\left(\frac{\Omega t}{3}\right) \right], \quad (43)$$

Into equation (40), using appropriate trigonometric identities to simplify nonlinear terms, collecting coefficients of similar harmonics, ignoring harmonic terms greater than the fundamental, and setting the coefficients of different remaining harmonics to zero, leads to the following set of coupled non-linear algebraic equations:

$\cos(\Omega t)$:

$$\left[1 - \Omega^2 - \varepsilon_1 \Omega^2 \left(\frac{19}{36} A_1^2 + \frac{4}{9} A_{1/3}^2 + \frac{2}{3} B_{1/3}^2 \right) + \varepsilon_2 \left(\frac{3}{4} A_1^2 + \frac{3}{2} A_{1/3}^2 + \frac{3}{2} B_{1/3}^2 \right) \right] A_1 + \varepsilon_1 \Omega^2 \left(\frac{1}{6} A_{1/3} B_{1/3}^2 - \frac{1}{18} A_{1/3}^3 \right) + \varepsilon_2 \left(\frac{1}{4} A_{1/3}^3 - \frac{3}{4} A_{1/3} B_{1/3}^2 \right) = P \cos \phi \quad (44)$$

$\sin(\Omega t)$:

$$-\delta \Omega A_1 + \varepsilon_1 \Omega^2 \left(\frac{1}{18} B_{1/3}^3 - \frac{1}{6} A_{1/3}^2 B_{1/3} \right) + \varepsilon_2 \left(\frac{3}{4} A_{1/3}^2 B_{1/3} - \frac{1}{4} B_{1/3}^3 \right) = P \sin \phi \quad (45)$$

$\cos\left(\frac{\Omega t}{3}\right)$:

$$\left[1 - \frac{1}{9} \Omega^2 - \frac{5}{9} \varepsilon_1 \Omega^2 + \varepsilon_2 \left(\frac{3}{2} A_1^2 + \frac{1}{4} B_{1/3}^2 \right) \right] A_{1/3} + \left(\frac{3}{4} \varepsilon_2 - \frac{1}{6} \varepsilon_1 \Omega^2 \right) A_1 A_{1/3}^2 + \left(\frac{3}{4} \varepsilon_2 - \frac{1}{18} \varepsilon_1 \Omega^2 \right) A_{1/3}^3 = -\frac{1}{3} \delta \Omega B_{1/3} - \frac{1}{6} \varepsilon_1 A_1 B_{1/3}^2 + \varepsilon_2 \left(\frac{1}{4} A_1^2 B_{1/3} + \frac{1}{2} A_1 B_{1/3}^2 \right) \quad (46)$$

$\sin\left(\frac{\Omega t}{3}\right)$:

$$\left[1 - \frac{1}{9} \Omega^2 + \varepsilon_1 \Omega^2 \left(\frac{1}{3} A_1 A_{1/3} - \frac{1}{18} A_{1/3}^2 - \frac{5}{9} A_1^2 \right) + \varepsilon_2 \left(\frac{3}{2} A_1^2 - \frac{2}{3} A_1 A_{1/3} + \frac{3}{4} A_{1/3}^2 \right) \right] B_{1/3} + \left(\frac{3}{4} \varepsilon_2 - \frac{1}{18} \varepsilon_1 \Omega^2 \right) B_{1/3}^3 = \frac{1}{3} \delta \Omega A_{1/3}.$$

(47)

The above four nonlinear coupled algebraic equations has four unknown constants

$A_1, A_{1/3}, B_{1/3}$ and ϕ . These equations can be reduced to three in the

constants $A_1, A_{1/3}, B_{1/3}$, by adding the square of equations (44) and (45) to eliminate the phase ϕ . This leads to the following equation, written in a form appropriate for a particular numerical procedure illustrated shortly:

$$A_1^2 + b_1 A_1 + b_2 = 0 \quad (48)$$

Where

$$b_1 = \frac{2(b_3 b_4 + b_5 b_6)}{b_3^2 + b_5^2}, \quad b_2 = \frac{b_4^2 + b_6^2 - P^2}{b_3^2 + b_5^2}$$

$$b_3 = \left[1 - \Omega^2 - \varepsilon_1 \Omega^2 \left(\frac{19}{36} A_1^2 + \frac{4}{9} A_{1/3}^2 + \frac{2}{3} B_{1/3}^2 \right) + \varepsilon_2 \left(\frac{3}{4} A_1^2 + \frac{3}{2} A_{1/3}^2 + \frac{3}{2} B_{1/3}^2 \right) \right],$$

$$b_4 = \varepsilon_1 \Omega^2 \left(\frac{1}{6} A_{1/3} B_{1/3}^2 - \frac{1}{18} A_{1/3}^3 \right) + \varepsilon_2 \left(\frac{1}{4} A_{1/3}^3 - \frac{3}{4} A_{1/3} B_{1/3}^2 \right)$$

$$b_5 = -\delta \Omega, \quad b_6 = \varepsilon_1 \Omega^2 \left(\frac{1}{18} B_{1/3}^3 - \frac{1}{6} A_{1/3}^2 B_{1/3} \right) + \varepsilon_2 \left(\frac{3}{4} A_{1/3}^2 B_{1/3} - \frac{1}{4} B_{1/3}^3 \right) \quad (49)$$

Equations (46)-(48) are three nonlinear coupled algebraic equations which, for given system parameters, can only be solved numerically for the three unknown harmonic coefficients $A_1, A_{1/3}$ and $B_{1/3}$ in these equations. A numerical solution to these equations can be carried out using any of the several well known methods of nonlinear coupled algebraic equations solving techniques such as Newton- Raphson method available in the MATLAB nonlinear algebraic equations toolbox. In the present work these equations were solved by a direct iterative technique which uses an appropriate implicit form of these equations. It is noted that in the 1/3 sub-harmonic resonance region, based on results of other investigators for other oscillators [2, 3, 27],

$B_{1/3} < 1$, $A_1 \approx \frac{-9P}{8\Omega^2}$ and $A_1, B_{1/3} \ll A_{1/3}$; in fact some investigators obtained sub-

harmonic approximate solutions for Duffing type oscillators assuming $A_1 = \frac{-9P}{8\Omega^2}$, i.e.

[2,3]. Taking these facts into consideration, equations (47) and (48) are solved implicitly for, respectively, $B_{1/3}$ and A_1 :

$$B_{1/3} = \frac{c_0}{c_1 + c_2 B_{1/3}^2} \quad (50)$$

$$A_1 = -\frac{b_2}{A_1 + b_1} \quad (51)$$

Where b_1, b_2 are as defined in equations (49). Also, noting that the 1/3 sub-harmonic resonance, in addition to the trivial solution, has two branches, and then equation (46) was rewritten in the implicit quadratic form:

$$A_{1/3}^2 + d_1 A_{1/3} + d_2 = 0,$$

The two roots of which are given by

$$A_{1/3} = \frac{1}{2} \left[-d_1 \pm (d_1^2 - 4d_2)^{1/2} \right] \quad (52)$$

Where

$$d_1 = \frac{d_4}{d_5}, \quad d_2 = \frac{\left(d_3 - \frac{d_6}{A_{1/3}} \right)}{d_5}, \quad d_3 = \left[1 - \frac{1}{9} \Omega^2 - \frac{5}{9} \varepsilon_1 \Omega^2 + \varepsilon_2 \left(\frac{3}{2} A_1^2 + \frac{1}{4} B_{1/3}^2 \right) \right],$$

$$d_4 = \left(\frac{3}{4} \varepsilon_2 - \frac{1}{6} \varepsilon_1 \Omega^2 \right) A_1, \quad d_5 = \left(\frac{3}{4} \varepsilon_2 - \frac{1}{18} \varepsilon_1 \Omega^2 \right),$$

$$d_6 = -\frac{1}{3} \delta \Omega B_{1/3} - \frac{1}{6} \varepsilon_1 A_1 B_{1/3}^2 + \varepsilon_2 \left(\frac{1}{4} A_1^2 B_{1/3} + \frac{1}{2} A_1 B_{1/3}^2 \right). \quad (54)$$

Equations (50)-(52) were solved with a direct iteration method, for given system parameters, using a specially written MATLAB program. The iteration started

with an initial guess for the variables A_1 , $A_{1/3}$ and $B_{1/3}$. The iteration process was stopped when, for each of the variables, the difference between the newly calculated value and one in the previous step is less than 10^{-5} . The total amplitude $a_{1/3}$ of the 1/3-subramonic steady state response is then calculated using the relation;

$$a_{1/3} = \left[A_{1/3}^2 + B_{1/3}^2 \right] \quad (55)$$

For convenience, the results obtained using the above HB solutions are presented and compared in chapter (6) with those obtained using the MMS and direct integration of equation (1).

3 Stability of harmonic balance solution

A local stability analysis of the harmonic balance approximate solution, presented in the previous section, for the 1/3 sub-harmonic resonance response of the oscillator in equation (1) can be performed by superposing a perturbation $v(t)$ on the steady state solution given by equation (41). That is, one lets:

$$u(t) = u_0(t) + v(t) \quad (56)$$

where $u_0(t)$ is given by equation (41) with coefficients as defined by equations (52)-(54), and $v(t)$ is a small variation in $u_0(t)$. Substituting equation (56) and its time derivatives into equation (2), using equation (41) and keeping only linear terms in v , one obtains the linearized variational Hill's type equation :

$$\begin{aligned}
& \left[1 + \frac{\varepsilon_1}{2} (A_1^2 + A_{1/3}^2 + B_{1/3}^2) + \varepsilon_1 \left(A_1 A_{1/3} + \frac{A_{1/3}^2}{2} - \frac{B_{1/3}^2}{2} \right) \cos\left(\frac{2\Omega t}{3}\right) + \varepsilon_1 A_1 A_{1/3} \cos\left(\frac{4\Omega t}{3}\right) \right. \\
& \left. + \varepsilon_1 (A_{1/3} B_{1/3} - A_1 B_{1/3}) \sin\left(\frac{2\Omega t}{3}\right) + \varepsilon_1 A_1 B_{1/3} \sin\left(\frac{4\Omega t}{3}\right) + \frac{\varepsilon_1 A_1^2}{2} \cos(2\Omega t) \right] \ddot{v} \\
& + \left[\delta + \frac{2}{3} \varepsilon_1 \Omega B_{1/3} (A_{1/3} - A_1) \cos\left(\frac{2\Omega t}{3}\right) + \frac{1}{3} \varepsilon_1 \Omega (B_{1/3}^2 - A_{1/3}^2 - A_1 A_{1/3}) \sin\left(\frac{2\Omega t}{3}\right) \right. \\
& \left. + \frac{4}{3} \varepsilon_1 \Omega A_1 \left(B_{1/3} \cos\left(\frac{4\Omega t}{3}\right) - A_{1/3} \sin\left(\frac{4\Omega t}{3}\right) - A_1 \sin(2\Omega t) \right) \right] \dot{v} \\
& + \left[1 - \varepsilon_1 \Omega^2 \left(\frac{A_1}{2} + \frac{A_{1/3}^3}{18} + \frac{B_{1/3}^2}{18} \right) + \frac{3}{2} \varepsilon_2 (A_1^2 + A_{1/3}^2 + B_{1/3}^2) + \right. \\
& \left[3\varepsilon_2 \left(A_1 A_{1/3} + \frac{A_{1/3}^2}{2} + \frac{B_{1/3}^2}{2} \right) - \frac{\varepsilon_1 \Omega^2}{6} \left(A_{1/3}^2 - B_{1/3}^2 + \frac{14}{3} A_1 A_{1/3} \right) \right] \cos\left(\frac{2\Omega t}{3}\right) \\
& + \left[3\varepsilon_2 B_{1/3} (A_{1/3} - A_1) - \frac{\varepsilon_1 \Omega^2 B_{1/3}}{9} (3A_{1/3} - 7A_1) \right] \sin\left(\frac{2\Omega t}{3}\right) \\
& + \left(3\varepsilon_2 A_1 A_{1/3} - \frac{7}{9} \varepsilon_1 \Omega^2 A_1 A_{1/3} \right) \cos\left(\frac{4\Omega t}{3}\right) + A_1 B_{1/3} \left(3\varepsilon_2 - \frac{13}{9} \varepsilon_1 \Omega^2 \right) \sin\left(\frac{4\Omega t}{3}\right) \\
& \left. + \frac{3}{2} A_1^2 (\varepsilon_2 - \varepsilon_1 \Omega^2) \cos(2\Omega t) \right] v = 0 \quad (57)
\end{aligned}$$

The above linear variational equation contains several parametric excitation terms which indicates that there are different possible scenarios by which the 1/3 sub-harmonic resonance can lose its stability. The uncovering of these different scenarios is rather involved and is beyond the scope of the present work. The focus of this work will be on the divergional (e.g. overflow) instability of the 1/3 the sub-harmonic resonance. For this purpose, using Floquet theory, the boundary between stable and unstable regions of the 1/3th sub-harmonic resonance solution is determined by assuming a particular solution to the variational equation (57) in the form [17, 27];

$$v(t) = C_1 \cos\left(\frac{\Omega t}{3}\right) + C_2 \sin\left(\frac{\Omega t}{3}\right)$$

(58)

Where C_1, C_2 are unknown constants. Then, upon substituting equation (57) into equation (57), and equating the coefficients of $\cos\left(\frac{\Omega t}{3}\right)$ and $\sin\left(\frac{\Omega t}{3}\right)$ in the resulting equation to zero, one obtains the set of coupled linear algebraic homogeneous equations in C_1 and C_2 :

$$\begin{bmatrix} \beta_{11} & \beta_{12} \\ \beta_{21} & \beta_{22} \end{bmatrix} \begin{Bmatrix} C_1 \\ C_2 \end{Bmatrix} = \begin{Bmatrix} 0 \\ 0 \end{Bmatrix} \quad (59)$$

Where

$$\beta_{11} = g_6 + \frac{g_7}{2} - \frac{\Omega^2}{18} g_2 - \frac{\Omega}{6} g_5 - \frac{\Omega^2}{9} g_1,$$

$$\beta_{12} = \frac{\Omega \delta}{3} + \frac{\Omega}{6} g_1 - \frac{\Omega^2}{18} g_3 + \frac{1}{2} g_8, \quad \beta_{21} = \frac{\Omega}{6} g_4 - \frac{\Omega^2}{18} g_3 + \frac{1}{2} g_8 - \frac{\Omega \delta}{3},$$

$$\beta_{22} = \frac{\Omega^2}{18} g_2 - \frac{\Omega^2}{9} g_1 + g_6 - \frac{1}{2} g_7 + \frac{\Omega}{6} g_5,$$

$$g_1 = 1 + \frac{\varepsilon_1}{2} (A_1^2 + A_{1/3}^2 + B_{1/3}^2), \quad g_2 = \varepsilon_1 (A_1 A_{1/3} + \frac{1}{2} A_{1/3}^2 - \frac{1}{2} B_{1/3}^2),$$

$$g_3 = \varepsilon_1 B_{1/3} (A_{1/3} - A_1), \quad g_4 = \frac{2}{3} \varepsilon_1 \Omega B_{1/3} (A_{1/3} - A_1),$$

$$g_5 = \frac{1}{3} \varepsilon_1 \Omega (B_{1/3}^2 - A_{1/3}^2 - 2A_1^2),$$

$$g_6 = 1 - \frac{1}{2} \varepsilon_1 \Omega^2 (A_1^2 + \frac{1}{9} A_{1/3}^2 + \frac{1}{9} B_{1/3}^2) + \frac{3}{2} \varepsilon_2 (A_1^2 + A_{1/3}^2 + B_{1/3}^2),$$

$$g_7 = \frac{3}{2} \varepsilon_2 (2A_1 A_{1/3} + A_{1/3}^2 + B_{1/3}^2) - \frac{1}{6} \varepsilon_1 \Omega^2 (A_{1/3}^2 - B_{1/3}^2 + \frac{21}{27} A_1 A_{1/3}),$$

$$g_8 = 3\varepsilon_2 B_{1/3} (A_{1/3} - A_1) - \frac{1}{3} \varepsilon_1 \Omega^2 B_{1/3} (A_{1/3} - \frac{21}{9} A_1). \quad (60)$$

Nontrivial solutions for C_1 and C_2 requires that the characteristic determinant, denoted by Δ , in equation (59) be zero; that is, the boundary between stable and unstable regions is given by:

$$\Delta = \beta_{11}\beta_{22} - \beta_{12}\beta_{21} = 0 \quad (61)$$

Also, in the stable region $\Delta > 0$, while in the unstable region $\Delta < 0$, [17, 27]. For convenience, examples of the results obtained using the above stability analysis of the $1/3$ sub-harmonic resonance response of the oscillator in equation (41) are presented and discussed in the next chapter. All of the required computations in this analysis procedure were carried out using a specially constructed MATLAB program.

CHAOS DIAGNOSTIC TOOLS

There are a number of well developed diagnostic tools used for characterizing, visualizing and quantifying periodic, quasi-periodic, and chaotic oscillations in physical systems. Examples of the commonly used of these tools are: Lyapunov exponents, Poincare maps, topological dimensions, phase plane plots, and frequency spectra. Following is a brief description of these tools; more detailed and in-depth descriptions are found, among others, in [19-23].

1 Lyapunov exponents

Lyapunov exponents λ_j are a quantitative criterion for testing chaos. They represent a measure of the average rates of convergence or divergence of nearby orbits in phase space and thus represent a measure of the motion sensitivity to changes initial conditions. For a system represented by n - state equation which include the time t as a state variable, there are exactly n Lyapunov exponents $\lambda_j, j = 1, 2, \dots, n$, i.e. for the single degree of freedom forced oscillator under consideration given in equation (1), there are three state equations which include the time as a state variable, and thus there are three Lyapunov exponents. The set of *Lyapunov* exponents for a given system is defined as follows [23]:

$$\lambda_j = \lim_{t \rightarrow \infty} \left[\frac{1}{t} \log_2 \left(\frac{r_j(t)}{r_j(0)} \right) \right], \quad j = 1, 2, \dots, n$$

$$\lambda_1 \geq \lambda_2 \geq \dots \geq \lambda_n$$

where $r_j(t)$ measures the growth, under the dynamics of the system, of a small n -sphere of initial conditions in the system n -dimensional phase space at $t = 0$ in terms of the j -th ellipsoidal axis. A positive Lyapunov exponent implies chaotic motion. Thus, in practice, one computes the largest Lyapunov exponent of the steady state motion (e.g., after allowing sufficient time for the transient response to die out) to determine whether this motion is or is not chaotic. An excellent and commonly used numerical procedure for calculating the full spectrum of Lyapunov exponents $\lambda_j, j = 1, 2, \dots, n$ from a generated time series (i.e. time history of motion generated by numerically integrating the system equation of motion) has been developed by Wolf et al [23]. In the present work, the Software which uses this numerical procedure will be used to calculate the Lyapunov exponents for steady state response of the oscillator in equation (1).

It noted that the full spectrum of Lyapunov exponents $\lambda_j, j = 1, 2, \dots, n$, order as a sequence $\lambda_1 \geq \lambda_2 \geq \dots \geq \lambda_n$, allows one, using the theorem listed bellow and other relevant ones (see, e.g., [37]), to get more information about the type of the motion attractor involved.

Theorem 1.

$\lambda_j = 0$ for at least one j , for any limit set that is not an equilibrium point.

Theorem 2.

$\sum_{j=1}^n \lambda_j < 0$ for any dissipative system.

Theorem 3.

$\lambda_j < 0$ for $j=1, \dots, n, \Rightarrow$ the attractor is a stable equilibrium

$\lambda_1 = 0$ and $\lambda_j, j = 2, n \Rightarrow$ the attractor is a stable limit cycle

$\lambda_1 = \lambda_2 = 0$ and $\lambda_j, j = 3, n \Rightarrow$ the attractor is a stable two-torus

$\lambda_1 = \dots = \lambda_k = 0$ and $\lambda_j, j = k + 1, n \Rightarrow$ the attractor is a stable K-torus

$\lambda_1 > 0 \Rightarrow$ the attractor is a chaotic.

Based on the above, for the three-dimensional non-conservative oscillator considered

in the present work, the motion is chaotic if $\lambda_1 > 0$, $\lambda_2 = 0$ and $\lambda_3 < 0$, with $\sum_1^3 \lambda_j < 0$.

It is noted that the above theorems are also used to exclude the possibility of chaos in one and two-dimensional systems, e.g., the dimension of a dynamic system must at least be three to have a chaotic motion. Also it is noted that there is a number of measures of the topological dimensions of a motion attractor [19-22], e.g., Lyapunov dimension, correlation dimension, information dimension, capacity and Hausdorff dimension. In many cases these different measures yield approximately the same value for the topological dimension of the considered attractor. With the availability of Lyapunov exponents, one can easily calculate the Lyapunov dimension d_L , which is given by [23];

$$d_L = K + \frac{\sum_{j=1}^K \lambda_j}{|\lambda_{K+1}|}$$

where the integer K is defined by the conditions:

$$\sum_{j=1}^K \lambda_j > 0, \text{ and } \sum_{j=1}^{K+1} \lambda_j < 0.$$

2 Phase Planes Orbits

The Phase plane plot is a simple graphical method for distinguishing periodic motions from non-periodic ones. Motions for second-order systems. A phase plane analysis can be used to study motion trajectories for various initial conditions, for stability decision and for limit cycles detection. To generate the phase plane plots, first the system equations of motion are written as a set of n -autonomous first order differential equations, where n is number of system state variables that span the phase space which, for the non-autonomous system include the time as a state variable. In the phase space plot, time is implicit, and trajectories represent solutions to the system state equations. The phase plane is obtained by plotting two of the system state space variables (i.e. displacement and velocity (or momentum)) versus each other, that is, the phase plane is a two dimensional projection of the phase space , spanning two arbitrary state variables. For the present non-autonomous oscillator in equation (1) the phase plane plots are plots of u vs. \dot{u} . Key features of the phase plane plots for non-autonomous single degree of freedom oscillators, such as the present one in equation (1), are the following:

- 1- A periodic motion traces a closed orbit
- 2- A k - period sub-harmonic motion traces a closed orbit that crosses itself k times
- 3- Quasi-periodic and chaotic motions both fill –up the area of the phase plane.

It is noted that the phase plane method is limited in its usage for systems up to second order inclusive because application of this method to higher-order systems is graphically complex.

3 Poincare' maps

A Poincare' map is a useful tool in the analysis of the motion of a nonlinear dynamic response. It allows one to distinguish between different types of periodic motion, between periodic and nonperiodic motions, and between chaotic and nonchaotic motions. To construct a Poincare' map, one constructs a hyper surface (called Poincare' section) in the state space that is transverse to the flow (trajectory) of the given system state equations. For an n -D autonomous system, the hyper-surface dimension is less than n . for an n -D non-autonomous system (which includes time as a state variable), the dimension of a Poincare' section is $n-1$, also each point in this hyper surface is specified by $n-1$ coordinates corresponding to the $n-1$ system state variables used to construct the system phase space. A Poincare' map is then constructed by sampling at an appropriate rate the successive intersections of a system trajectory in the phase space with the constructed, one sided, Poincare' section. Thus, a Poincare' map is a transformation (map) that maps the current intersection to the subsequent one on a Poincare' section.

For the 3-D non-autonomous oscillator under consideration in the present work, given by equation (1), a Poincare' map is constructed by plotting in the (u, \dot{u}) the sequence of sampled points $(u(t_k), \dot{u}(t_k))$, $t_k = t_0 + KT$, $K=1,2, \dots$, where the sampling

time $T = \frac{2\pi}{\Omega}$ is the period of the harmonic forcing with frequency Ω , and t_0 is an arbitrary starting time of the sampling process; e.g. for analysis of the steady state response t_0 is chosen large enough to give sufficient time for the system transient response to die out. By examining the 2-D plot of a Poincare' map of a harmonically forced oscillator, such as the one under consideration in the present work, the following remarks can be made about the type of motion involved;

Poincare' Map

Motion Type

1-Single point	Harmonic motion at fundamental period T .
2-Finite K -points	Sub-harmonic motion of period KT .
3- Infinitely K -points filling up a closed curve	Quasi-periodic motion ;e.g two incommensurate frequencies present.
4- A cloud of unorganized points	Strange attractor: possibly chaotic, or quasi-periodic motion with three or more dominant incommensurate frequencies.

4 Frequency spectrum

Most numerical software packages, such as MATLAB, and experimental signal analysers include tools for computing the Fourier spectrum of a signal. The spectrum associated with an arbitrary state variable (e.g. displacement u of the oscillator in equation (1)) is a useful tool for distinguishing between periodic and non-periodic motion, and between chaotic and non-periodic motions of a harmonically driven nonlinear oscillator.

A periodic motion with fundamental frequency Ω displays a discrete frequency spectrum with spikes at $n\Omega$, $n \equiv \text{integer}$. A quasi-periodic motion also shows up as a discrete frequency spectrum displaying spikes at the incommensurate frequencies of the harmonics involved in the motion. A sub-harmonic period-3 motion, $T = \frac{2\pi}{\Omega}$, shows up as a discrete spectrum displaying spikes at $\frac{n\Omega}{3}$, $n = 1, 2, \dots$.

A Chaotic motion displays a continuous broad-band frequency spectrum with spikes at the dominating frequencies.

In the present work, the FFT of the steady state displacement $u(t)$ of the nonlinear oscillator in equation (1) was obtained using a specially constructed MATLAB program. The program uses the last 1024 discrete points of displacement $u(t)$ obtained by numerically integration equation (1), over about 1000 cycles of motion, using a 4th order Runge-Kutta method. In all of the cases considered, the last 1024 data point used in the FFT analysis included, in the frequency range considered, about 10-25 cycles of the oscillator motion $u(t)$.

RESULTS AND DISCUSSION OF RESULTS

The characteristics and stability of the 1/3 sub-harmonic resonance response curves of the harmonically forced nonlinear oscillator given in equation (1) where studied analytically and numerically over a selected range of the oscillator parameters: $\varepsilon_1, \varepsilon_2, \delta, P$ and Ω . The analytical study was based on the approximate first order MMS solutions given in equations (21) and (34), and the approximate two-mode harmonic balance (2MHB) solutions given in equations (50)-(52), and (61). The numerical solutions were obtained by integrating equation (1) using a 4-th order Runge-Kutta method. By examining the waveform of the displacement $u(t)$ for many trial runs, it was found that for the purpose of this work, an integration time $t=1000$ sec. with a step $\Delta t = 0.1$ sec. yields sufficiently accurate results and provides about 300 sec decay time for the transient part of the response. This transient time was found to be sufficient in all of the cases considered. Thus, the last 700sec of the obtained time series of the displacement $u(t)$ is considered to be the steady state response. The FFT analysis was carried out on the last 1024 of these points of the time series $u(t)$ which corresponds to a time duration of 102.4sec from $t=8977$ sec to $t= 1000$ sec of the steady state response. Thus, for the considered frequency range $1.5 \leq \Omega \leq 6$, the obtained FFT spectrum represents the frequency content of the steady state response for about 25-100 excitation cycles with period $T = \frac{2\pi}{\Omega}$ which corresponds to 7-33 cycles of a steady state $3T$ sub-harmonic response. The FFT spectrum of the steady state time series $u(t)$ provided the numerical solution for the amplitudes of the fundamental and that of the 1/3 sub-harmonic components of the steady state response.

The phase plane plot, Ponicare' map and Lyapunov exponents were obtained for the steady state response from $t=500\text{sec}$ to $t=1000\text{sec}$.

It is to be noted that, for given system parameters, there is a threshold value of forcing amplitude P , (which strongly depends on damping ratio δ), below which a $1/3$ sub-harmonic resonance of the oscillator in equation (1) is not possible. In order to numerically generate a sub-harmonic solution, when it exists, the initial conditions in the numerical integration procedure have to be within the domain of attraction of the sub-harmonic steady state solution. In the present work, the MMS and 2MHB approximate solutions were used to provide initial conditions for the numerical integration. This, to some extent, reduced the elaborate search in the state space for the domain of attraction for stable and unstable sub-harmonic solutions. The stability of the approximate analytic solutions was determined by comparing them with the numerically obtained results; that is, a numerical solution starting at the predicted theoretical values was considered unstable if it diverges away from these values and settles into a different solution.

Examples of results simulation for typical steady state responses obtained using the approximate analytical solutions and numerical procedures indicated above are depicted in figures (1)-(21). In all of the cases presented in these figures the value of ε in equation (1) was taken as unity, e.g. $\varepsilon = 1$.

Figures (1)-(5) show examples of the effects of forcing amplitude P , damping ratio δ and initial conditions on the onset of the $1/3$ sub-harmonic resonance.

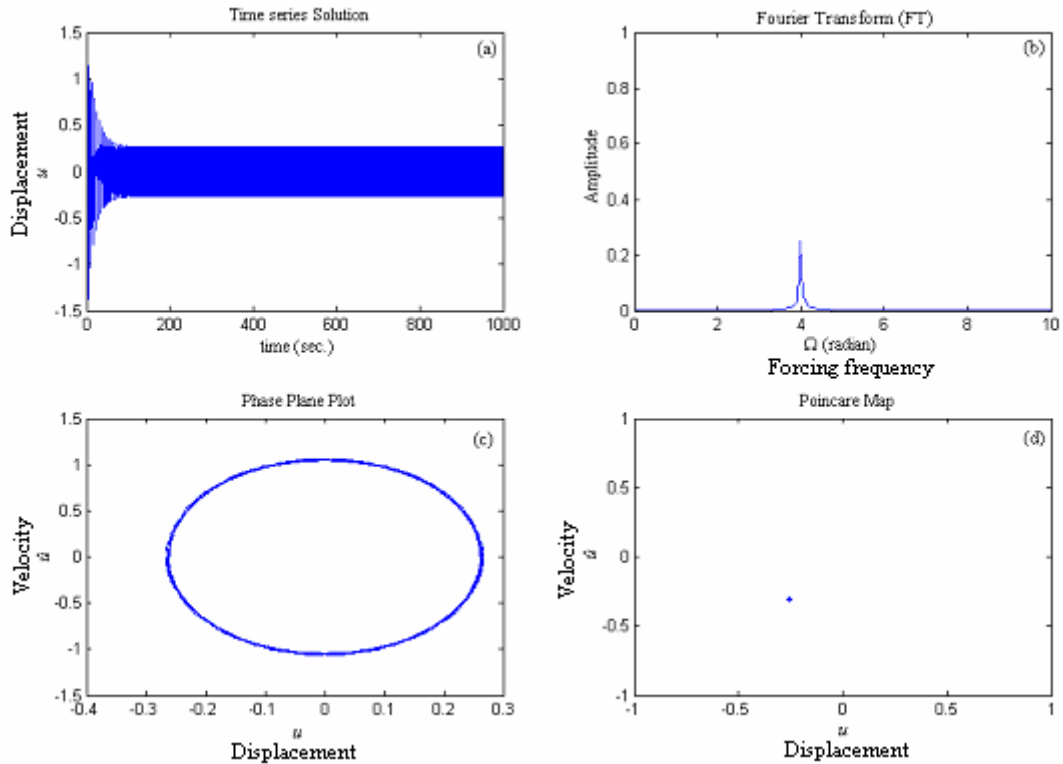


Fig. (1) : Numerical solution : (a) : Time series solution (b) : Fourier transform
(c) : Phase plane plot (d) : Poincare' map.

$$\varepsilon = 1, \varepsilon_1 = 0, \varepsilon_2 = 0.1, \delta = 0.1, P = 4, \Omega = 4, u(0) = 1, \dot{u}(0) = 0.$$

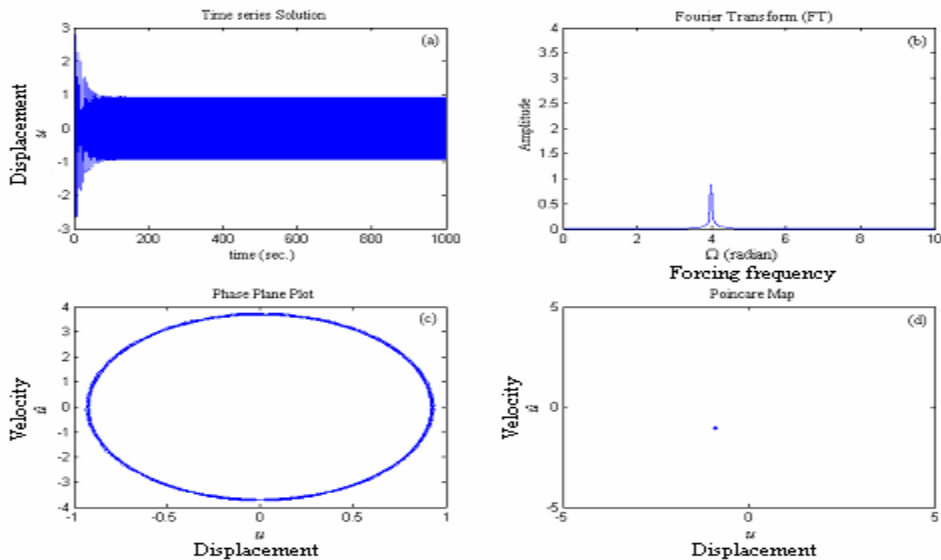


Fig. (2) : Numerical solution : (a) : Time series solution (b) : Fourier transform
(c) : Phase plane plot (d) : Poincare' map.

$$\varepsilon = 1, \varepsilon_1 = 0, \varepsilon_2 = 0.1, \delta = 0.1, P = 14, \Omega = 4, u(0) = 1, \dot{u}(0) = 0.$$

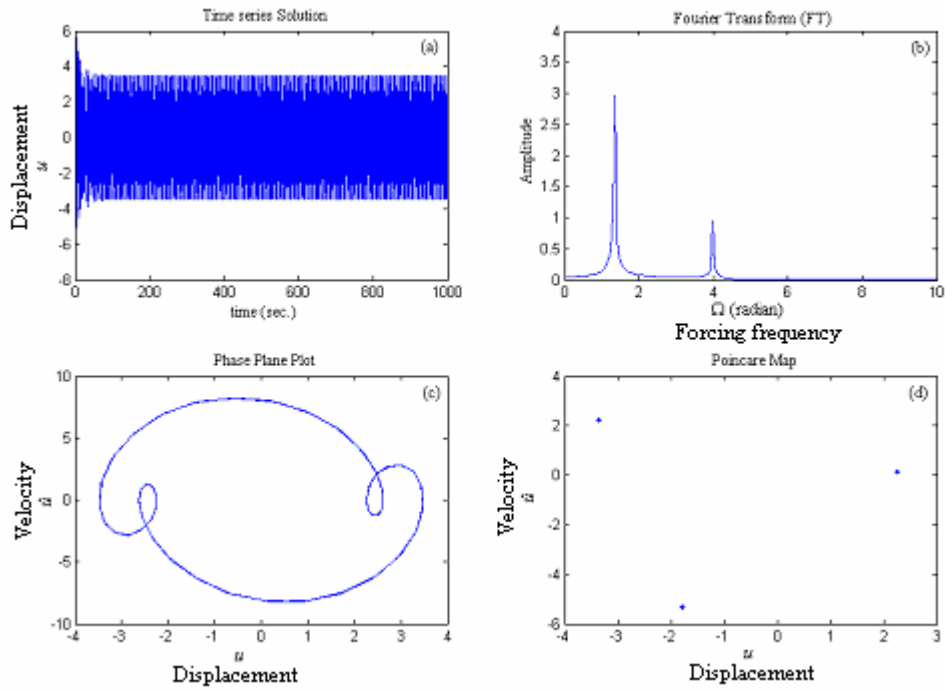


Fig. (3) : Numerical solution : (a) : Time series solution (b) : Fourier transform
 (c) : Phase plane plot (d) : Poincare' map.
 $\varepsilon = 1, \varepsilon_1 = 0, \varepsilon_2 = 0.1, \delta = 0.1, P = 14, \Omega = 4, u(0) = 5, \dot{u}(0) = 0.$

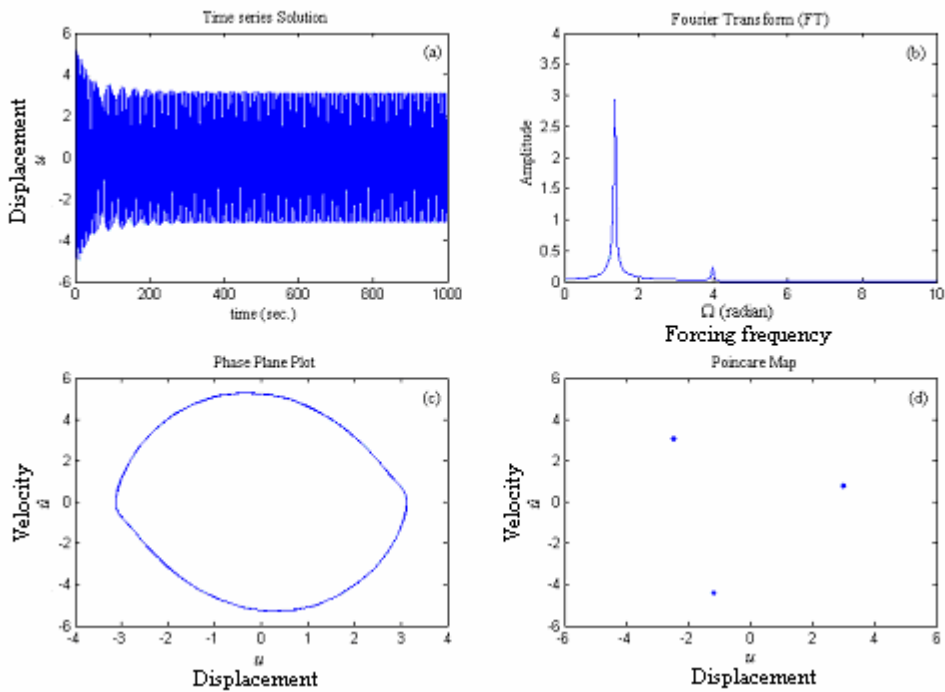


Fig. (4) : Numerical solution : (a) : Time series solution (b) : Fourier transform
 (c) : Phase plane plot (d) : Poincare' map.
 $\varepsilon = 1, \varepsilon_1 = 0, \varepsilon_2 = 0.1, \delta = 0.02, P = 4, \Omega = 4, u(0) = 5, \dot{u}(0) = 0.$

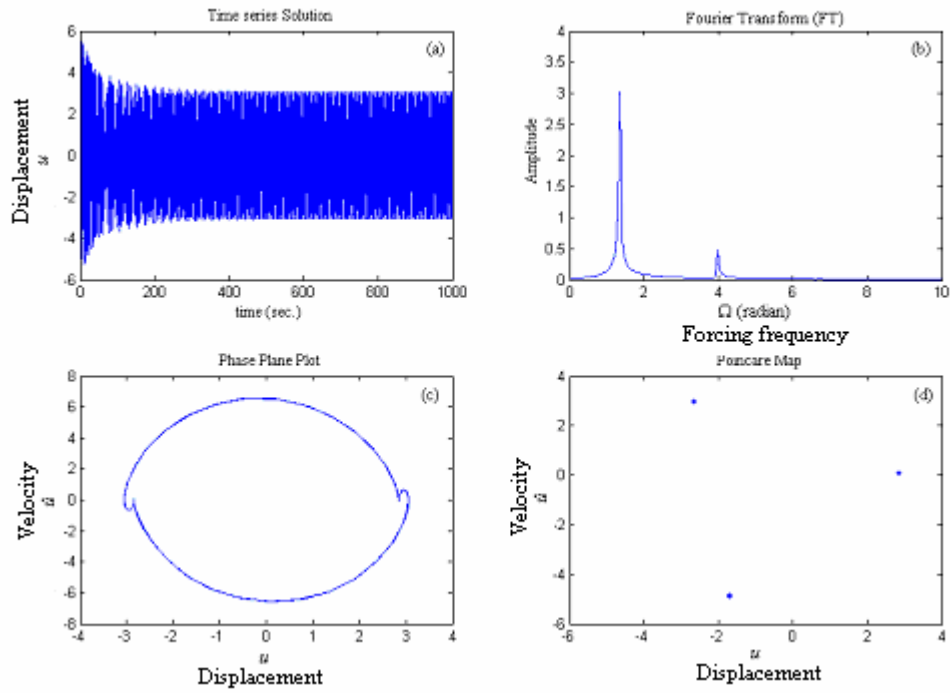


Fig. (5) : Numerical solution : (a) : Time series solution (b) : Fourier transform
(c) : Phase plane plot (d) : Poincaré' map.

$$\varepsilon = 1, \varepsilon_1 = 0, \varepsilon_2 = 0.1, \delta = 0.02, P = 8, \Omega = 4, u(0) = 5, \dot{u}(0) = 0.$$

Figures (6)-(9) present typical results of comparisons between MMS and 2MHB approximate solutions, and between these solutions and results of numerical integration for cases where the hardening nonlinearity dominates (e.g. $\varepsilon_1 \ll \varepsilon_2$), hardening and softening nonlinearities have nearly equal strength (e.g. $\varepsilon_1 \approx \varepsilon_2$), and softening nonlinearity dominates ($\varepsilon_1 \gg \varepsilon_2$).

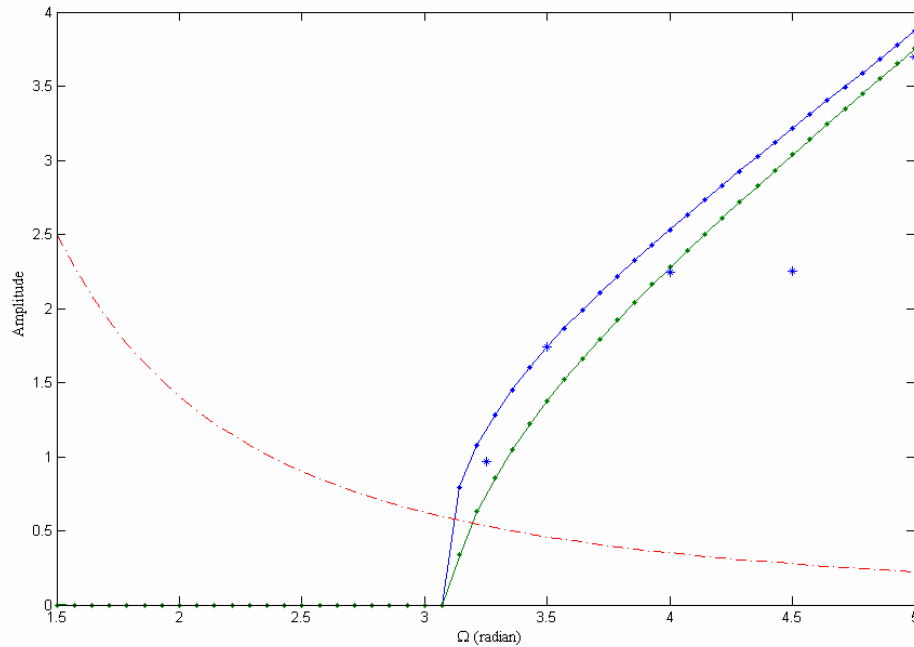


Fig.(6) : MMS, 2MHB and Numerical solution : (—) : 2MHB solution, (.) : MMS solution, (*) : Numerical solution, (—.) : Fundamental amplitude (A_1)(2MHB).
 $\varepsilon = 1$, $\varepsilon_1 = 0.02$, $\varepsilon_2 = 0.2$, $\delta = 0.01$, $P = 5$.

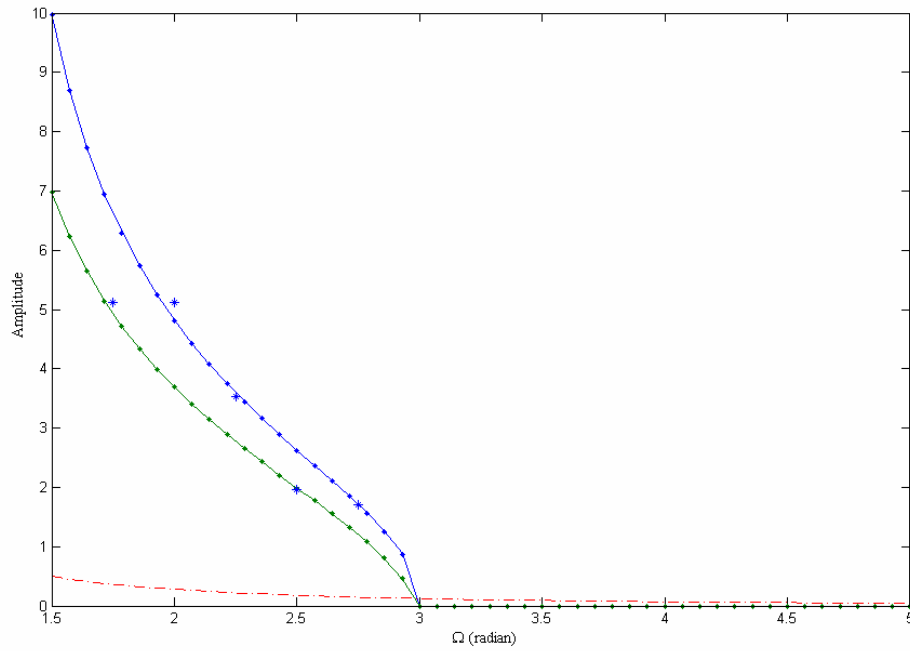


Fig.(7) : MMS, 2MHB and Numerical solution : (–) : 2MHB solution, (.) : MMS solution, (*) : Numerical solution, (–.) : Fundamental amplitude (A_1)(2MHB).
 $\varepsilon = 1$, $\varepsilon_1 = 0.2$, $\varepsilon_2 = 0.02$, $\delta = 0.01$, $P = 1$.

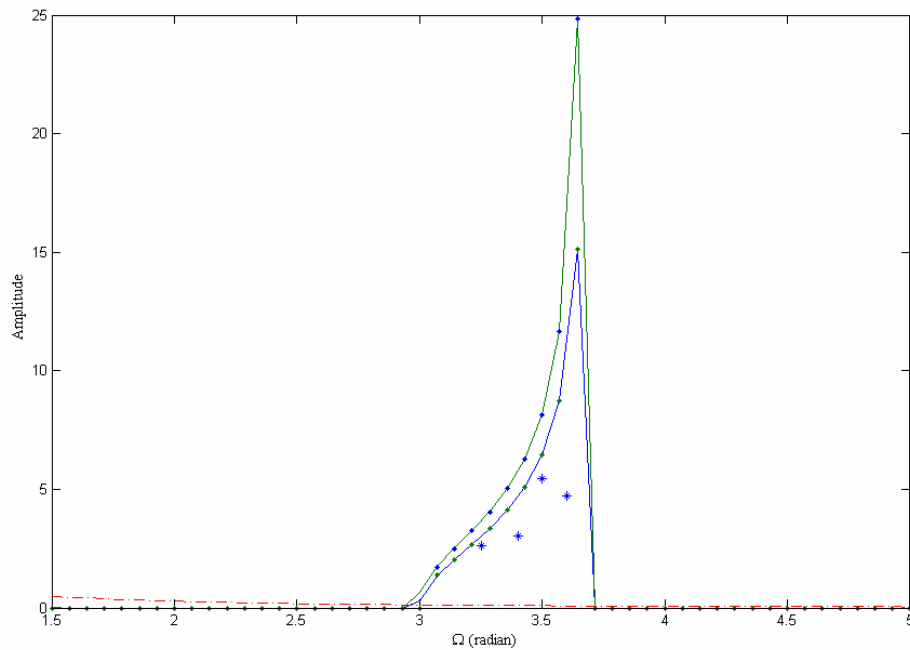


Fig.(8) : MMS, 2MHB and Numerical solution : (–) : 2MHB solution, (.) : MMS solution, (*) : Numerical solution, (–.) : Fundamental amplitude (A_1)(2MHB).
 $\varepsilon = 1$, $\varepsilon_1 = 0.1$, $\varepsilon_2 = 0.1$, $\delta = 0.01$, $P = 1$.

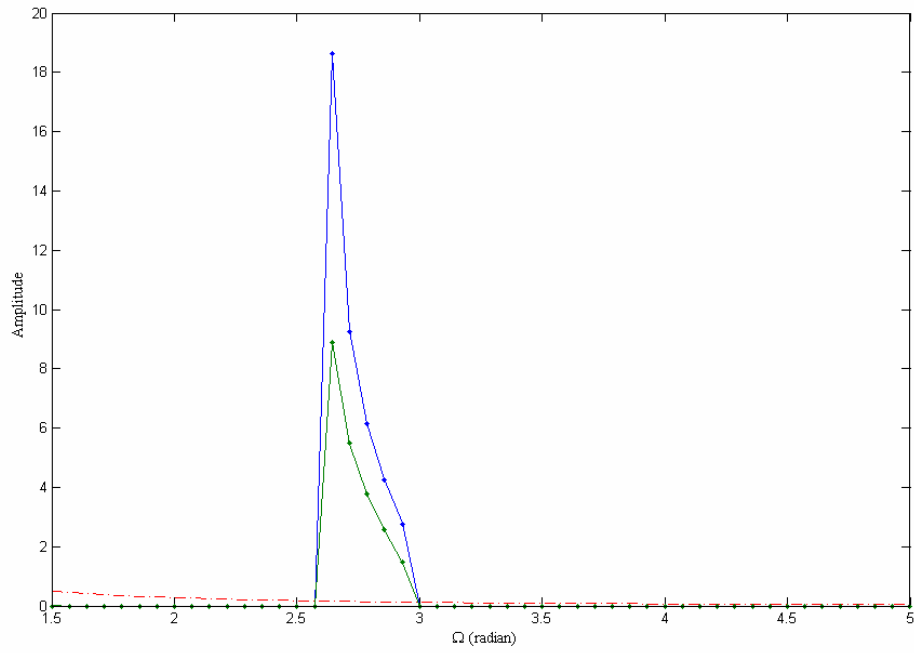


Fig.(9): MMS, 2MHB and Numerical solution : (-) : 2MHB solution, (.) : MMS solution, (*) : Numerical solution, (-.) : Fundamental amplitude (A_1)(2MHB).
 $\varepsilon = 1$, $\varepsilon_1 = 0.1$, $\varepsilon_2 = 0.05$, $\delta = 0.01$, $P = 1$.

Figures (10)-(15) display examples of the stability analysis results of the approximate MMS and HB solutions.

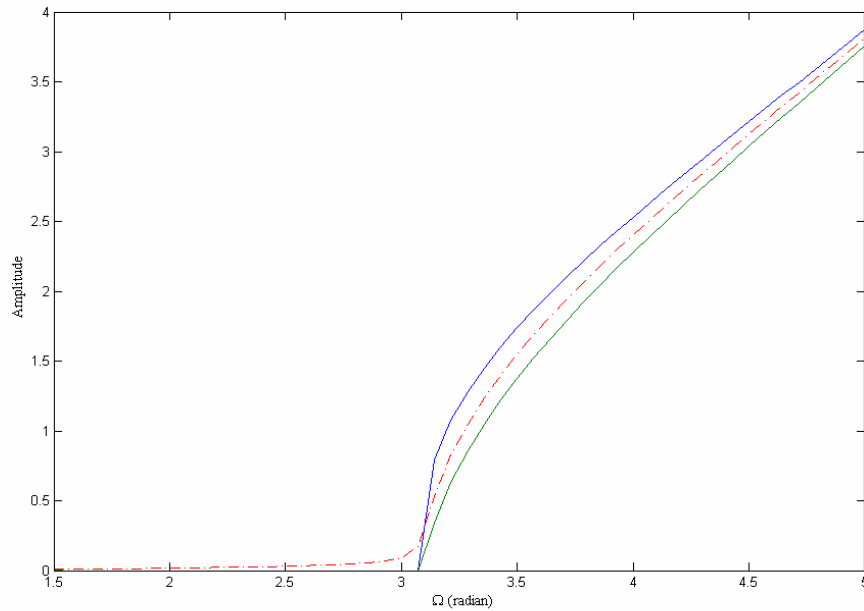


Fig.(10) : Approximate (MMS) results : (-) : MMS solution, (-.) : Stability curve.
 $\varepsilon = 1, \varepsilon_1 = 0.02, \varepsilon_2 = 0.2, \delta = 0.01, P = 5.$

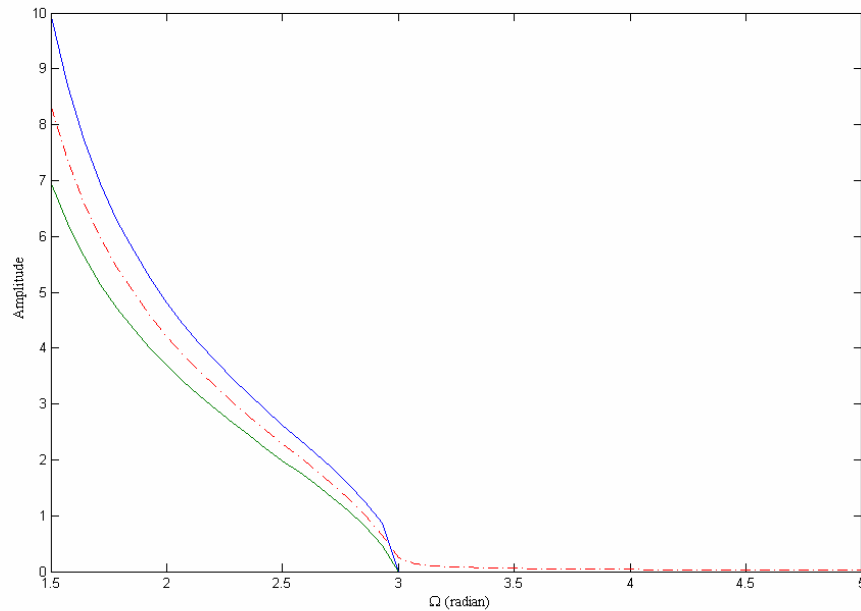


Fig.(11) : Approximate (MMS) results : (-) : MMS solution, (-.) : Stability curve.
 $\varepsilon = 1, \varepsilon_1 = 0.2, \varepsilon_2 = 0.02, \delta = 0.01, P = 1.$

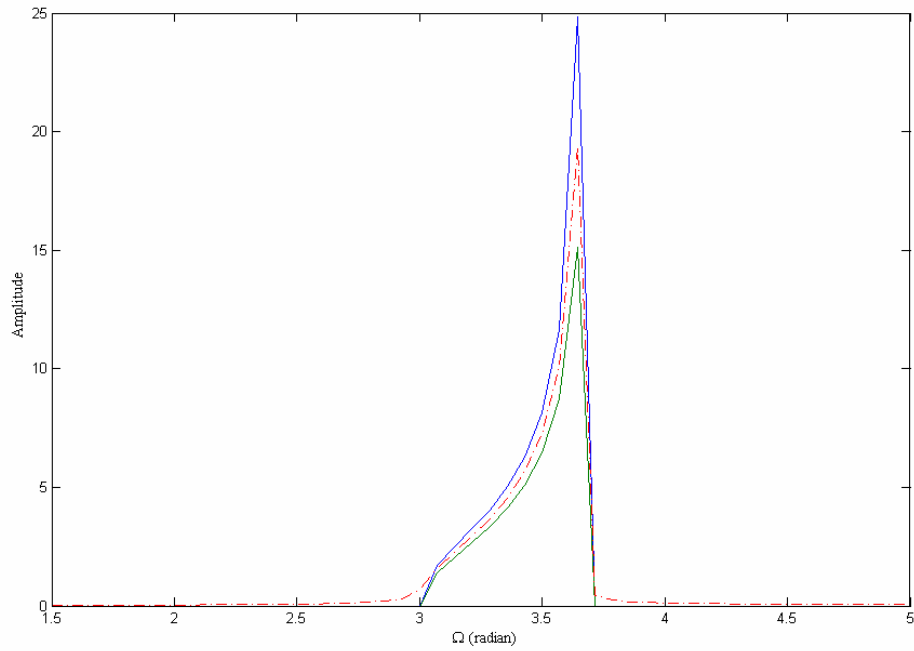


Fig.(12) : Approximate MMS solution : (—) : MMS solution, (---) : Stability curve.
 $\varepsilon = 1, \varepsilon_1 = 0.1, \varepsilon_2 = 0.1, \delta = 0.01, P = 1.$

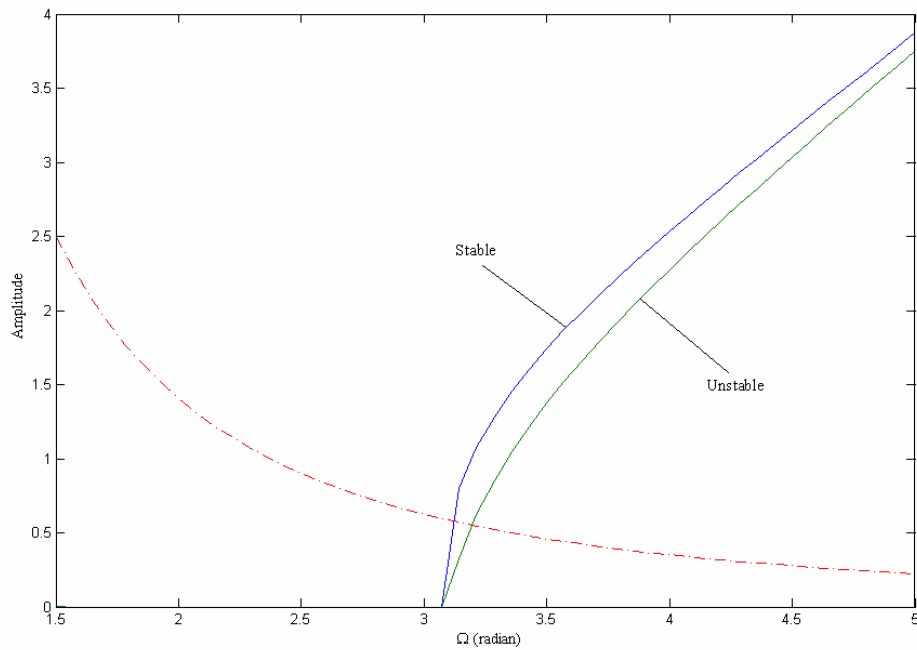


Fig.(13) : Approximate 2MHB solution : (—) : 2MHB solution,
 (---) : Fundamental amplitude (A_1)(2MHB solution).
 $\varepsilon = 1, \varepsilon_1 = 0.2, \varepsilon_2 = 0.02, \delta = 0.01, P = 5.$

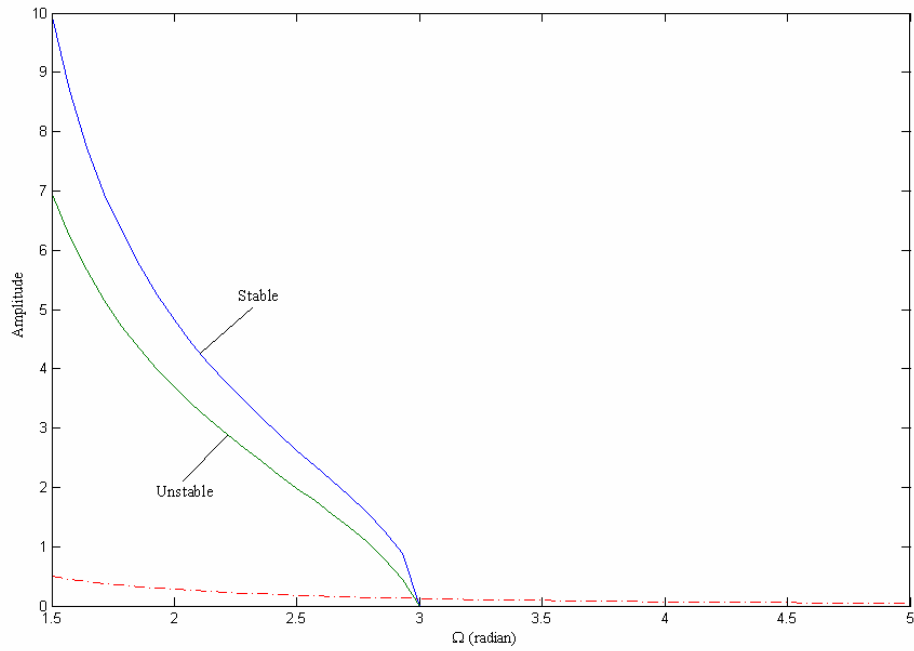


Fig.(14) : Approximate 2MHB solution : (-) : 2MHB solution,
 (-) : Fundamental amplitude (A_1)(2MHB solution).
 $\varepsilon = 1, \varepsilon_1 = 0.02, \varepsilon_2 = 0.2, \delta = 0.01, P = 1$.

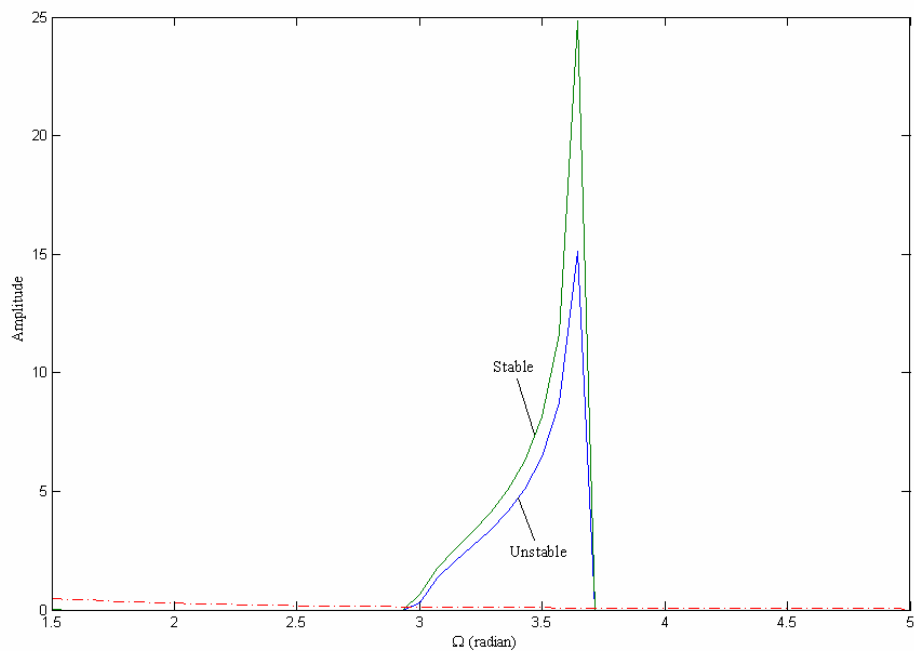


Fig.(15) : Approximate 2MHB solution : (-) : 2MHB solution,
 (-) : Fundamental amplitude (A_1)(2MHB solution).
 $\varepsilon = 1, \varepsilon_1 = 0.1, \varepsilon_2 = 0.1, \delta = 0.01, P = 1$.

Figures (16)-(21) show examples of the numerical simulation results obtained using the chaos analysis tools : phase plane plot, FFT spectrum, Poincare' map and Lyapunov exponents.

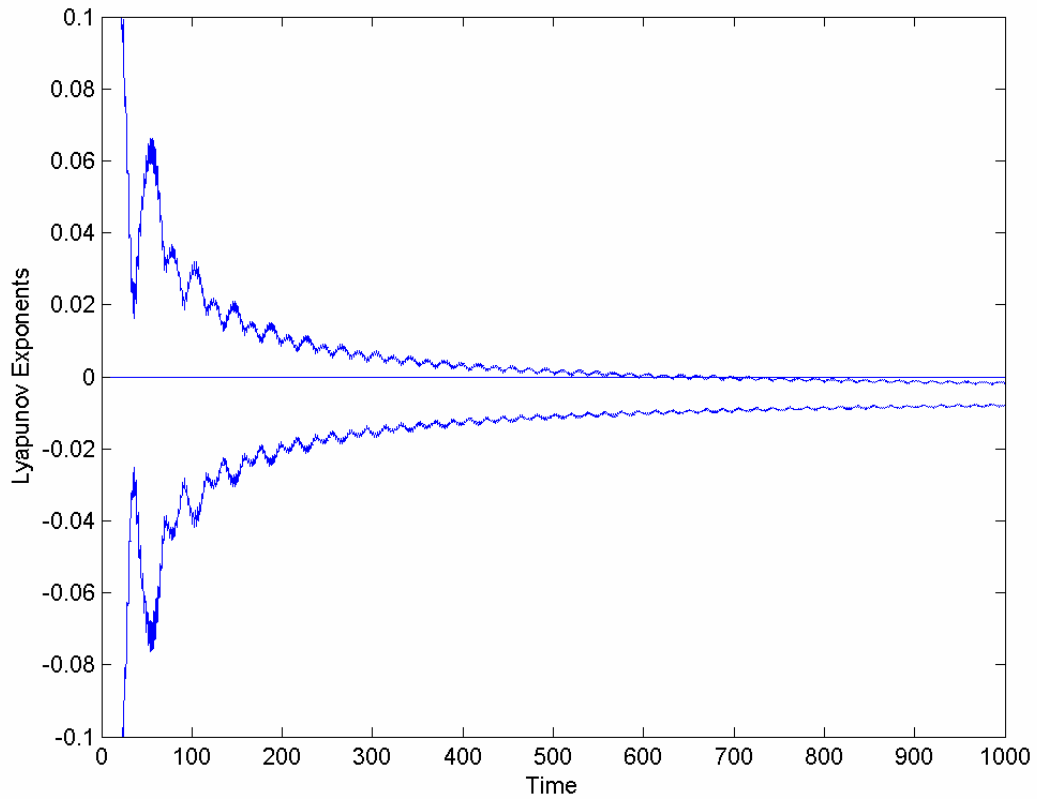


Fig.(16) : Lyapunov exponents. $\varepsilon = 1$, $\varepsilon_1 = 0.02$, $\varepsilon_2 = 0.2$, $\delta = 0.01$, $P = 5$, $\Omega = 3.5$,
 $u(0) = 1.75$, $\dot{u}(0) = 0$.

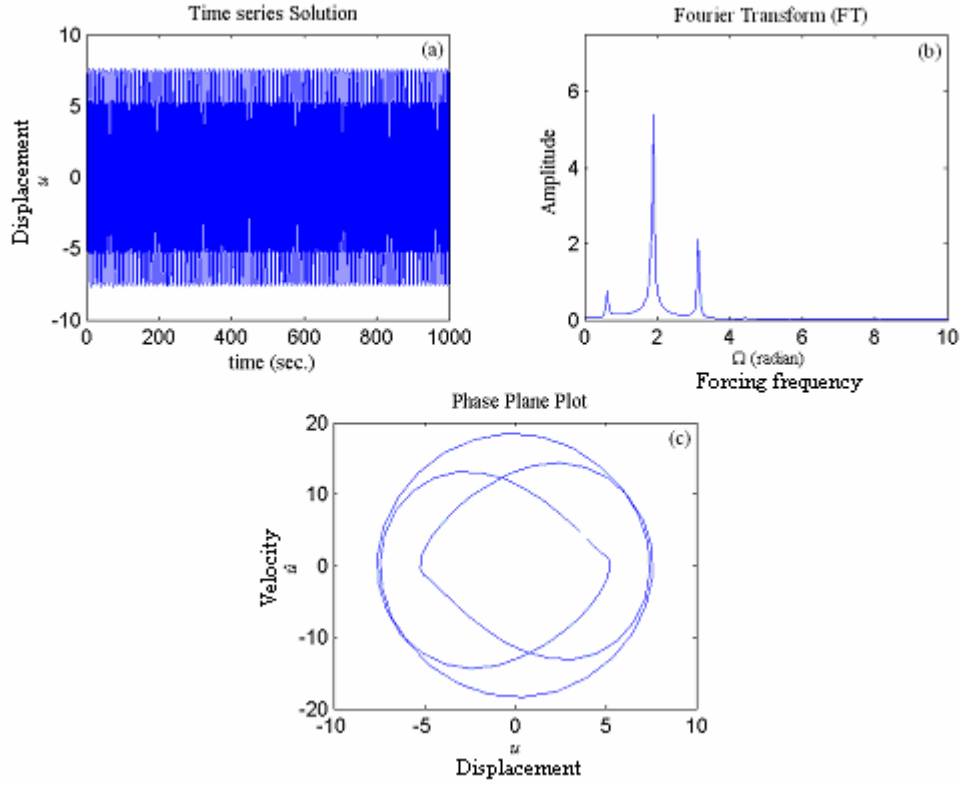


Fig. (17) : Numerical solution : (a) : Time series solution (b) : Fourier transform (c) : Phase plane plot.

$$\varepsilon = 1, \varepsilon_1 = 0.01, \varepsilon_2 = 0.1, \delta = 0.01, P = 14, \Omega = 3.14, u(0) = 5, \dot{u}(0) = 1.$$

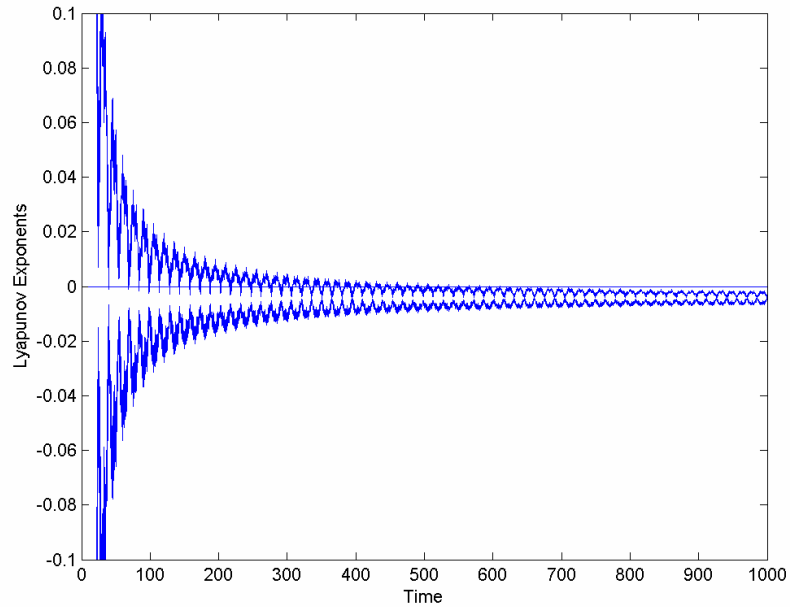


Fig.(17 - d) : Lyapunov exponents. $\varepsilon = 1, \varepsilon_1 = 0.01, \varepsilon_2 = 0.1, \delta = 0.01, P = 14, \Omega = 3.14, u(0) = 5, \dot{u}(0) = 1.$

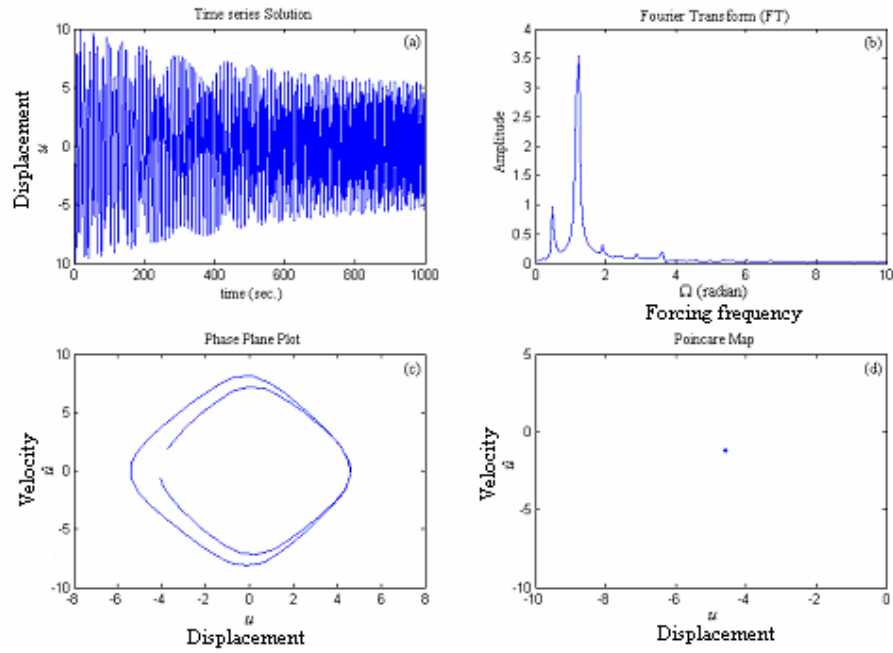


Fig. (18) : Numerical solution : (a) : Time series solution (b) : Fourier transform
(c) : Phase plane plot (d) : Poincare' map.

$$\varepsilon = 1, \varepsilon_1 = 0.1, \varepsilon_2 = 0.02, \delta = 0.01, P = 8, \Omega = 1.2, u(0) = 5, \dot{u}(0) = 1$$

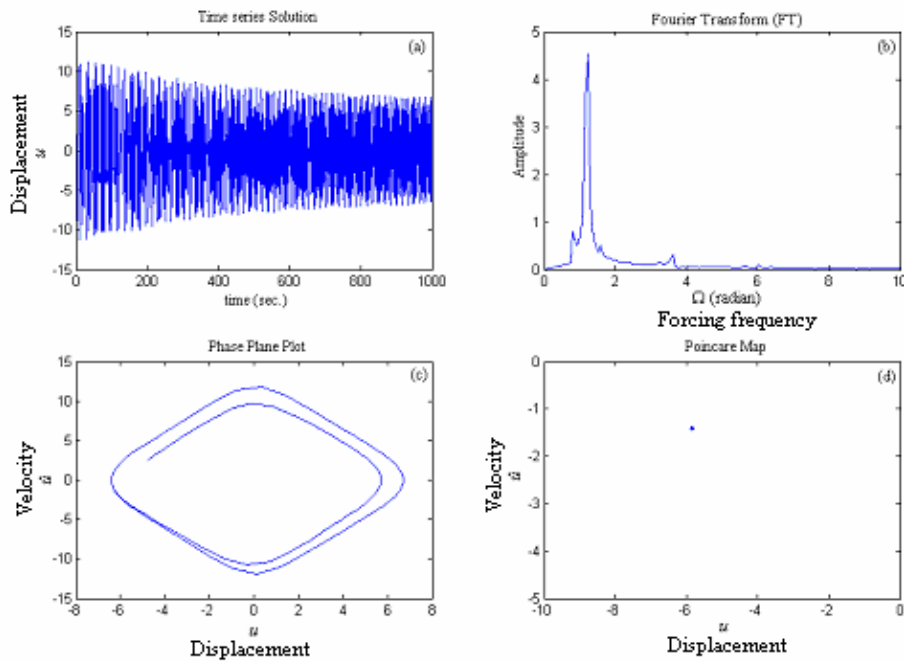


Fig. (19) : Numerical solution : (a) : Time series solution (b) : Fourier transform
(c) : Phase plane plot (d) : Poincare' map.

$$\varepsilon = 1, \varepsilon_1 = 0.1, \varepsilon_2 = 0.05, \delta = 0.01, P = 9, \Omega = 1.2, u(0) = 4, \dot{u}(0) = 1$$

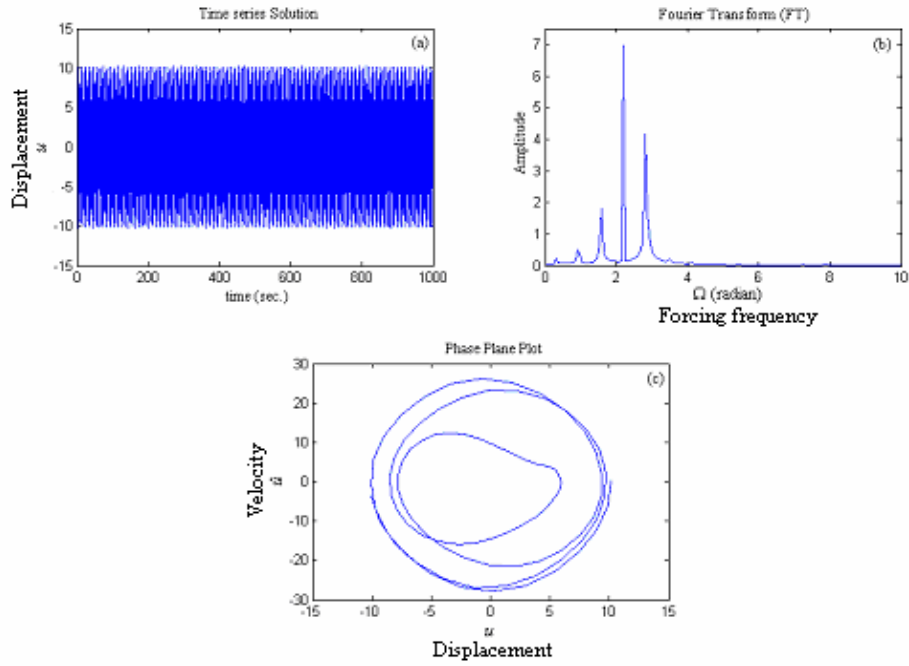


Fig. (20) : Numerical solution : (a) : Time series solution (b) : Fourier transform (c) : Phase plane plot .

$$\varepsilon = 1, \varepsilon_1 = 0.01, \varepsilon_2 = 0.1, \delta = 0.01, P = 14, \Omega = 2.84, u(0) = 5, \dot{u}(0) = 5$$

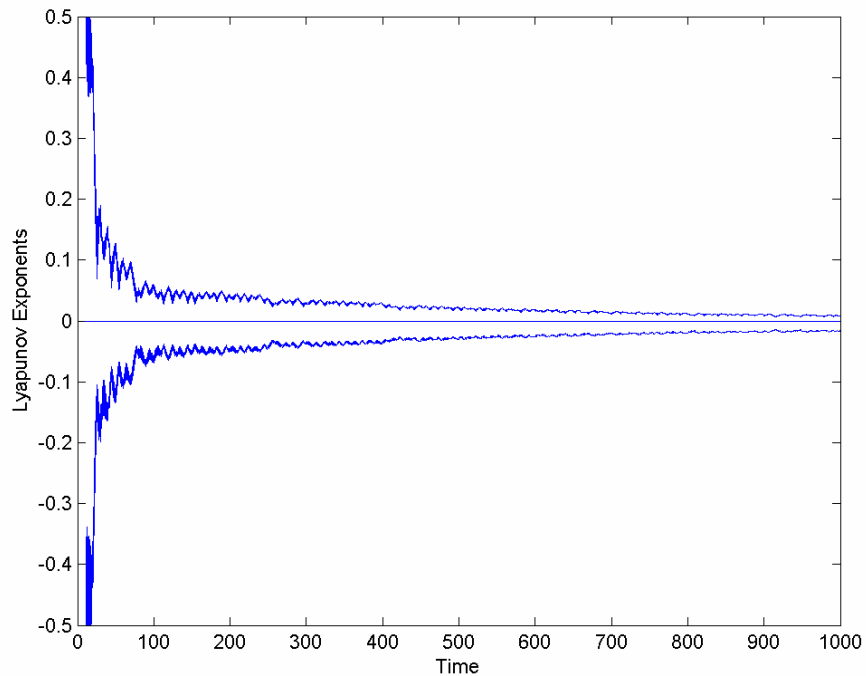


Fig.(20 - d) : Lyapunov exponents. $\varepsilon = 1, \varepsilon_1 = 0.01, \varepsilon_2 = 0.1, \delta = 0.01, P = 14, \Omega = 2.84, u(0) = 5, \dot{u}(0) = 5$.

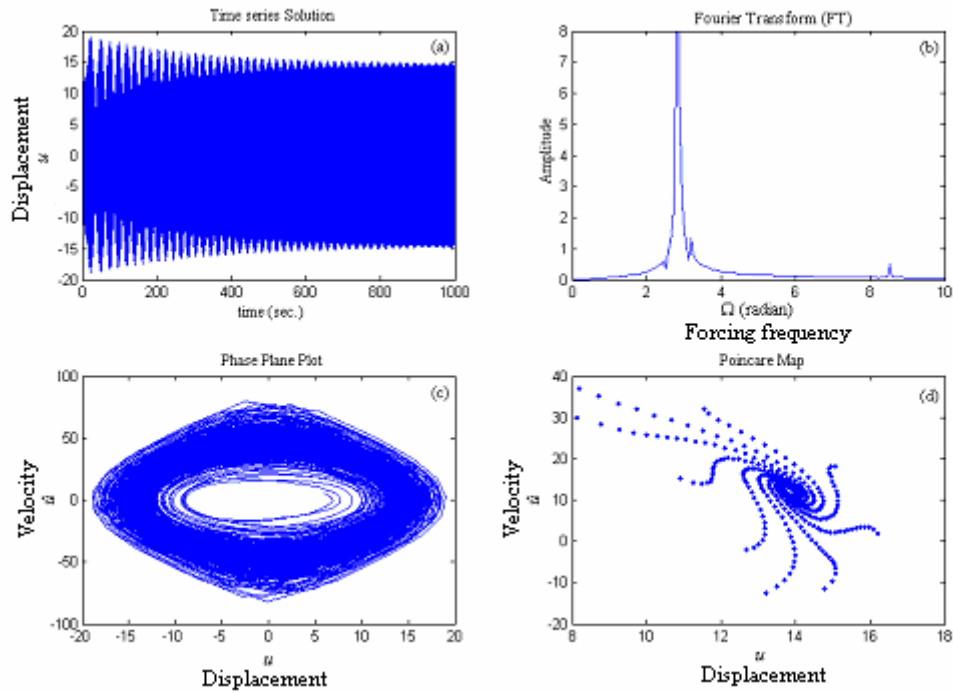


Fig. (21) : Numerical solution : (a) : Time series solution (b) : Fourier transform
(c) : Phase plane plot (d) : Poincare' map.

$$\varepsilon = 1, \varepsilon_1 = 0.01, \varepsilon_2 = 0.1, \delta = 0.01, P = 14, \Omega = 2.843, u(0) = 6, \dot{u}(0) = 5$$

Based on the results presented in these figures, the following remarks can be made about the 1/3 sub-harmonic resonance, and chaotic response of the present oscillator given in equation (1):

1. The sub-harmonic resonance is a bifurcation phenomenon: it is initiated as system parameters go through critical values. In the present oscillator, for given parameters $\varepsilon_1, \varepsilon_2$, there is a threshold value of forcing P below which, and a threshold value of damping δ above which, the 1/3 sub-harmonic resonance does not take place.
2. For given system parameters for which the sub-harmonic resonance exists, the initial conditions play a critical role in its onset; that is, in order for the steady

state to settle into the $1/3$ sub-harmonic attractor, the initial conditions have to be within the domain of attraction of this attractor.

3. Approximate first order MMS and approximate two modes 2MHB solutions yield, for the range of system parameters considered in this work (e.g. for the cases where the oscillator in equation (1) is weakly nonlinear) nearly identical prediction of the $1/3$ sub-harmonic resonance response of this oscillator. Their prediction accuracy, in comparison with that of numerical integration results, is qualitatively fair and quantitatively reasonably good for the cases where the oscillator is weakly nonlinear. For the cases where the oscillator is moderately or strongly nonlinear the accuracy of both of these approximate solutions is poor both qualitatively and quantitatively.
4. For the cases where the nonlinearities in the oscillator behaviour in equation (1) predominantly of the hardening type (e.g. $\varepsilon_1 \ll \varepsilon_2$) the $1/3$ sub-harmonic resonance, if exists (e.g. if $P > P_{critical}$, $\delta < \delta_{critical}$), is initiated at an excitation frequency $\Omega_c \geq 3\omega$, where ω is the natural frequency of the corresponding linear oscillator (for the present oscillator $\omega = 1$). This initiation value of Ω appears to move to right of the point 3ω as P and/or δ is increased, and the resonance curve show the typical hardening, e.g. bending to right, behaviour.
5. As ε_1 is increased from a value relatively low in comparison with that of ε_2 , the value Ω_c at which $1/3$ sub-harmonic resonance is initiated appears to move from a point to the right and towards $\Omega = 3\omega$. Increasing ε_1 further, while keeping ε_2 constant, the initiation point Ω_c continues to move towards the point $\Omega = 3\omega$ as P is increased and/or δ is decreased. As the softening and hardening nonlinearities in the oscillator behaviour in equation (1) become of

nearly equal strength (e.g. $\varepsilon_1 \approx \varepsilon_2$) the 1/3 sub-harmonic resonance, if exists (e.g. if $P > P_{critical}$, $\delta < \delta_{critical}$), is initiated at a point $\Omega_c < 3\omega$, and its curves have little or nearly no bending to either right or left (e.g. they resemble a linear oscillator of resonance curve) and have relatively large amplitude even for a relatively low value of forcing amplitude P . Despite their resembles to a linear oscillator resonance curve, the 1/3 sub-harmonic resonance curves still have two distinct (one upper and one lower) branches which do not coalesce like those of the hardening or softening cases.

6. For the cases where the softening nonlinearities in the oscillator in equation (1) are predominately of the softening type (e.g. $\varepsilon_1 \gg \varepsilon_2$) the 1/3 sub-harmonic resonance curves bend to left and exit only for $\Omega < 3\omega$. Starting at an excitation frequency Ω slightly above the linear natural frequency ω , a 1/3 sub-harmonic resonance of the predominately softening oscillator of relatively large amplitude, if exists (e.g. if $P > P_{cc}$, $\delta < \delta_{cc}$), is excited in a sub-critical as Ω is gradually increased. The amplitude of these resonance curves tend to decrease monotonically with increasing excitation frequency and eventually coalesce on the Ω axis at an excitation frequency Ω_c slightly below $\Omega = 3\omega$. For excitation frequency $\Omega \geq \Omega_c$ the 1/3 sub-harmonic resonance curves disappear. It is noted in this case of predominately softening behaviour the amplitude of the fundamental response A_1 can becomes comparable to that of the excited 1/3 sub-harmonic resonance as Ω enter the primary resonance, e.g. when Ω is decreased to a value well bellow 3ω and approaches ω . Generally speaking, $\Omega \approx < 1.5\omega$, the oscillator begins to exhibit complicated behaviours as the 1/3 sub-harmonic attractor may coexist with the

primary , sub-harmonics of order other than $1/3$, and chaotic attractors. In this case , the approximate solutions appear to breakdown; also the results of the numerical solutions become difficult to interpret when this numerical simulation is not carried out thoroughly and is not guided by more reliable approximate analytic solutions. For this reason, the data in all the presented figures where for excitation frequency $\Omega \geq 1.5 \omega$, ($\omega = 1$) and values of P and δ for which the fundamental amplitude is small in comparison with that of the excited $1/3$ sub harmonic response.

7. The stability analyses of the obtained MMS and 2MHB solutions indicate that the upper branch of the $1/3$ sub-harmonic resonance curves is stable and the lower one is unstable. This result agrees with that presented in [1]. These results indicate that chaotic behaviour of the present oscillator is likely to appear in a narrow zone between the primary and $1/3$ sub-harmonic zone, which is in agreement with the results presented in. Also, these results indicate that the softening oscillator (e.g. the case $\varepsilon_1 \gg \varepsilon_2$) is more susceptible to chaotic and aperiodic responses than the hardening one ($\varepsilon_1 \ll \varepsilon_2$) at the point. Also for the softening case, this chaotic response can occur in the primary frequency region (e.g. Ω not far from ω) while for the hardening type, the chaos appears to occur away from primary resonance (e.g. Ω close to 3ω).
8. The present results show that approximate analytic solutions aided with numerical methods such as phase plane plots, Poincare' map, FFT spectra, and Lyapunov exponents can be effective in studying complicated dynamic behaviours of harmonically forced single degree of freedom nonlinear oscillators.

RECOMMENDATIONS

The present study used first order MMS, and two modes harmonic balance 2MHB solutions and their stability analyses to study the 1/3 sub-harmonic response of the oscillator in equation (1). The analytical approximate solutions were aided with well known numerical simulation methods, namely phase plane plots, Poincare' maps, FFT spectra, Lyapunov spectra and direct numerical integration. The decay time used in the numerical simulations was about 300sec. The presented results indicated that the present oscillator have rich dynamics specially in the softening cases which cant be uncovered using first order approximate solutions and a decay time of 300sec; i.e. a decay time of 4000 time may be needed to realistically capture a chaotic attractor.

In light of results and conclusions discussed in the previous chapter, a further extension of the present investigation into the steady state behavior of the oscillator given in equation (1) may consider the following:

1. Obtaining approximate 2nd order MMS solution and higher order HB solutions to the 1/3 sub-harmonic resonance response
2. Performing more though stability and bifurcation analyses of the obtained higher order approximate solutions.
3. Allowing a much longer, say 4000 or more seconds, of transient time.
4. Obtaining approximate asymmetric solutions in addition to the symmetric ones considered in this work and studying other order (e.g. 1/2) sub-harmonic resonances especially for the softening case.
5. Presenting more detailed studies of the chaotic zones and the rout to chaos(such as period doubling).

REFERENCES

- A. A. Al-Qaisia and M. N. Hamdan (1999). On the Steady State Response of Oscillators with Static and Inertia Nonlinearities. **Journal of Sound and Vibration**, 223, 49-71.
- A. AL-Qaisia and M. N. Hamdan (2001), Bifurcations of Approximate Harmonic Balance Solutions and Transition to Chaos in an Oscillator with Inertial and Elastic Symmetric Nonlinearities. **Journal of Sound and Vibration**, 244, 453-479.
- A. AL-Qaisia and M. N. Hamdan (2002), Bifurcations and Chaos of an Immersed Cantilever Beam in a fluid and Carrying an Intermediate Mass. **Journal of Sound and Vibration**, 253, 853-888.
- A. H. Nayfeh and D. T. Mook (1979), **Nonlinear oscillations**, New York: John Wiley.
- A. H. Nayfeh and N. Balachandra (1995), **Applied Nonlinear Dynamics**. John Wiley: New York.
- A. Hassan and T. D. Burton (1995). Extraneous Solutions Predicted by the Harmonic Balance Method. **Journal of Sound and Vibration**, 182, 523-539.
- A. M. A. Hamdan , M. A. Nayfeh and A. H. Nayfeh (1989), The Effect of Nonlinearities on the Response of a Single-Machine-Quasi-Infinite- Busbar System. **IEEE Transactions on Power Systems**, PWRS-4- 843-849.
- A. Prosperetti (1976), Subharmonics and Ultraharmonics in Forced Oscillations of Weakly Nonlinear Systems. **Am. Journal of Physics**, 44, 548-554.

C. A. Ludeke (1951) Predominantly Subharmonic Oscillations. **Journal of Applied Physics**, 22, 1321-1328.

C. H. Hayashi (1953), Subharmonic Oscillations in Nonlinear Systems . **Journal of Applied Physics**, 24, 521-529.

C. H. Hayashi (1975), **Selected Papers on Nonlinear Oscillations**. Kyoto University.

C. H. Hayashi (1985), **Nonlinear Oscillations in Physical Systems**. Princeton University Press, Princeton, NJ

C. S. Hsu (1959), On Simple Subharmonics . **Quarterly of Applied Mathematics**, 17, 102-105.

D. W. Jordan and P. Smith (1977), **Non-linear Differential Equations**. New York: McGraw-Hill.

F. C. Moon (1987), **Chaotic Vibrations**. John Wiley and Sons: New York.

J. Guckenheimer and P. Holmes (1983), **Nonlinear Oscillations, Dynamical systems, and Bifurcations of Vector Fields**. Springer Verlag: New York Inc.

J. I. Stoker (1950) , **Nonlinear Vibrations in Mechanical and Electrical Systems**. Interscience, New York.

J. M. T. Thompson and P. Holmes (1987), **Nonlinear Dynamics and Chaos**. John Wiley and Sons : New York.

K. L. Janicki and W. Szemplinska-Stupnicka (1995), Subharmonic Resonances and Criteria for Escape and Chaos in a Driven Oscillator. **Journal of Sound and Vibration**, 180, 253-269.

K. L. Janicki and W. Szemplinska-Stupnicka (1997), Subharmonic Resonances in a Driven Oscillator: Bifurcation Structures and Transitions to Chaos. **European Journal of Mechanics and Solids**, 16, 671-694.

M. A. Nayfeh, A. M. A. Hamdan and A. H. Nayfeh (1991), Chaos and Instability in a power System: Subharmonic-Resonant Case. **Nonlinear Dynamics** 2, 53-72.

M. E. Levenson (1949), Harmonic and sub-harmonic response for the Duffing Equation. **Journal of Applied Physics**, 20, 1045-1055.

M. M. Stanisic and J. A. Euler (1973). General Perturbational Solution of a Harmonically Forced Nonlinear Oscillator. **International Journal of Nonlinear Mechanics**, 8, 523-538.

M. Mond, G. Cederbaum, P. B. Khan and Y. Zarmi (1993). Stability Analysis of the Nonlinear Mathieu Equation. **Journal of Sound and Vibration**, 167, 77-89.

M. N. Hamdan and B. O. Al- Bedoor (2001), Non-Linear Free Vibrations of a Rotating Flexible Arm. **Journal of Sound and Vibration**, 242,839-853.

M. N. Hamdan and M. H. F. Dado (1997) , Large Amplitude Free Vibrations of a Uniform Cantilever Beam Carrying an Intermediate Lumped Mass and Rotary Inertia. **Journal of Sound and Vibration**, 206, 151-168.

M. N. Hamdan and N. H. Shabaneh (1997) , On the Large Amplitude Free Vibrations of a Restrained Uniform Beam Carrying an Intermediate Lumped Mass. **Journal of Sound and Vibration**, 199, 711-736.

R. Riganti (1978) , Subharmonic Solutions of Duffing Equation with Large Nonlinearity, **International Journal of Nonlinear Mechanics**, 13, 21-31.

S. E. Newhouse (1980), Asymptotic Behavior and Homoclinic Points in Nonlinear Systems. **In Nonlinear Dynamics**, R. H. G. Helleman(ed). New York Academy of Science: New York.

S. Meazawa (1961), Steady Forced Vibrations of Unsymmetrical Piecewise Linear Systems. **Bull JSME** , 4, 200-209.

T. S. Parker and L. O. Chua (1989), **Practical Numerical Algorithms for Chaotic Systems**, Springer_Verlag: New York

W. Szemplinska-Stupnicka and J. Bajkowski (1986), The $1/2$ Subharmonic Resonance and its Transition to Chaotic Motion in a Nonlinear Oscillator. **International Journal of Nonlinear Mechanics**, 21, 401-419.

W. Szemplinska-Stupnicka (1987), Secondary Resonances and Approximate Models of Routes to Chaotic Motion in Non-Linear Oscillators. **Journal of Sound and Vibration**, 113, 155-172.

W.S. Loud (1972), Subharmonic Solutions of Second Order Equations Arising Near Harmonic Solutions. **Journal of Differential Equations**, 11, 628-660.

W. Wolf, J. B. Swift, H. L. Swinney and J. A. Vastano (1985), Determining Lyapunov Exponents From a Time Series. **Physica** **16D**, 285-317.

Y. Tsuda, J. Isoue, T. Tamura and A. Suoeka (1984). On the 1/2 Subharmonic resonance of a Nonlinear Vibrating System with a Hard Duffing Type Restoring Characteristics . **Bull JSME**, 27, 1280-1287.

Z. Rahman and T. D. Burton (1989), On higher Order Method of Multiple Scales in Non-Linear Oscillations- Periodic Steady State Response. **Journal of Sound and Vibration**, 133, 369-379.

الرنين التوافقي التحتي، استقراره وتشعبه وتحوله إلى العشوائية في المتذبذبات ذات الكسور الذاتي اللاخطي

إعداد

أشرف عبد المجيد الشالفة

المشرف

أ.د. محمد نادر حمدان

ملخص

يهدف هذا البحث نحو تطوير تقريبات تحليلية للرنين التوافقي التحتي من الدرجة (3/1)، ودراسة إستقراره، تشعبه وتحوله إلى العشوائية في المتذبذبات ذات الكسور الذاتي اللاخطي. وهنا سيكون الإهتمام في الحالات حيث تردد الإجبار حوالي ثلاثة أضعاف التردد الطبيعي الخطي. حيث سيحلل إستقرار الحلول التقريبية الناتجة وأن يمتحن البعد المختلط المحتمل ذو التشعيب الأحادي والانتقال إلى الفوضى في مستوى بمتغيرين لهذه الحلول التقريبية. وهناك عدد من الطرق العددية الأساسية-على سبيل المثال- تخطيطات الطور، خرائط بوينكار، أسس ليابانوف وأطياف التردد، ستستخدم للتأكد من صلاحية النتائج التحليلية التقريبية. وسيستخدم حل تحليلي تقريبي لأغراض المقارنة بطريقة HB و MMS وهذه النتائج التحليلية التقريبية المختلفة سيُقارن كل منها مع النتائج المحصلة باستخدام الطرق العددية المشهورة التي ذُكرت سابقاً.